Versatile photocatalytic activities of indenoquinoxalines for dye reduction, single crystal nucleation, and MNPs formation with Iron scrap under sunlight

Renu Kumari and Man Singh*

E-mail: renukumaribalot6@gmail.com ,*E-mail: mansingh50@hotmail.com .

School of Chemical Sciences, Central University of Gujarat, Gandhinagar, 382030, India.

*Corresponding author: Tel: +91-079-23260210; Fax: +91-079-23260076

Table of Contents

I. General Information

All the reagents were purchased from Sigma Aldrich. Structures were analyzed with ^{1}H, ^{13}C NMR, FT-IR, LC-MS, XRD, UV-Vis, HR-TEM, SEM, fluorescent spectroscopy, TGA, Raman spectroscopy, and elemental study were characterized.

2. Experimental procedures and compound characterization

Scheme S1. Synthesis of 11H-indeno[1,2-b] quinoxalin-11-one (IQ).

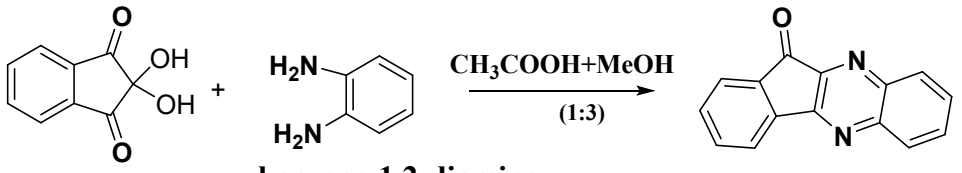

2,2-dihydroxy-1*H*-indene-1,3(2*H*)-dione + **benzene-1,2-diamine** → **11*H*-indeno[1,2-*b*]quinoxalin-11-one**

Table S1. Synthesis of IQ (**Scheme S1**).

Chemical Name	Mol. wt. (g)	mmol	Quantity(g)	Equivalent
benzene-1,2-diamine	108.1	11	1.1	1.1 eq
Ninhydrin	178.1	10	1.8	1.0 eq
Acetic acid	60.0		10.0 mL	
Methanol			30.0 mL	

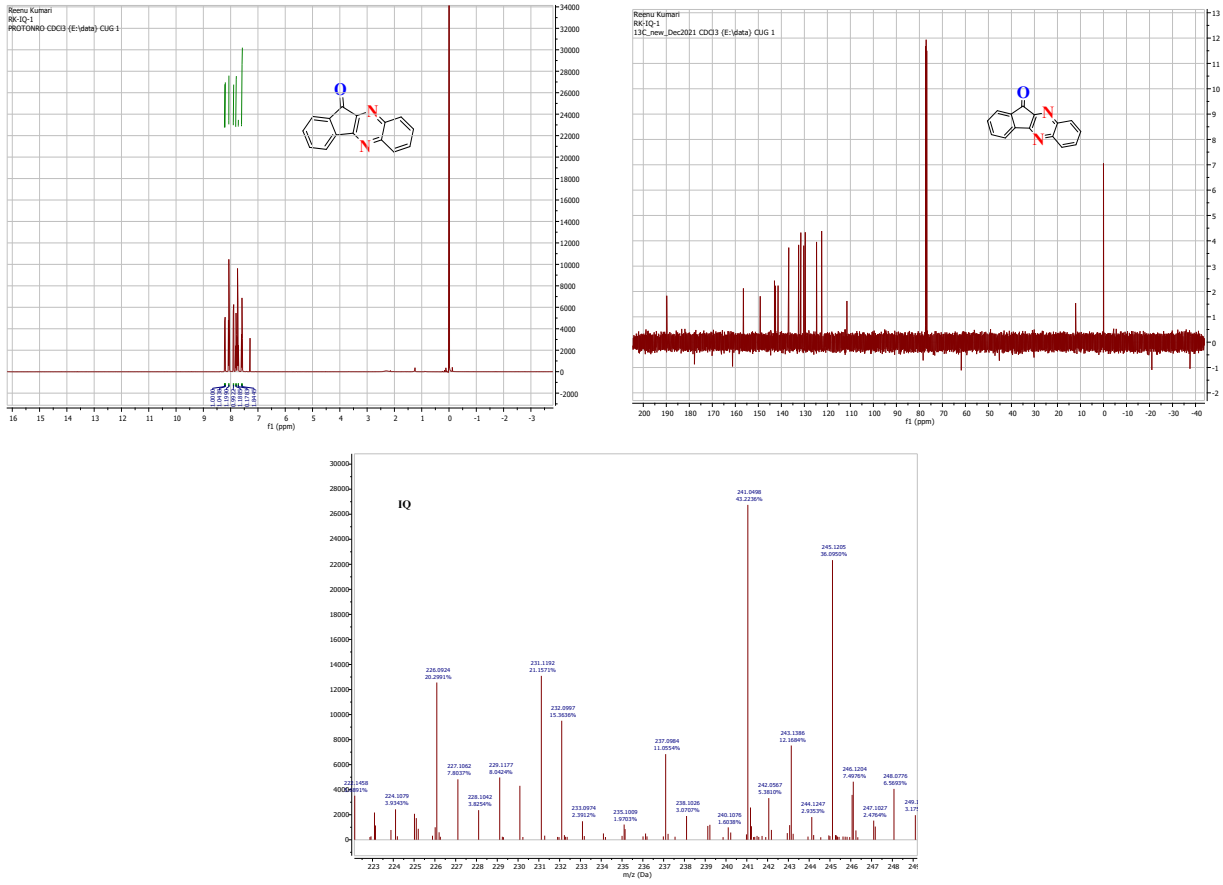

Fig S1. ^{1}H, ^{13}C NMR, and mass spectra for IQ (Scheme S1).

Light yellow solid, yield (91%), ^{1}H NMR 500 MHz ($CDCl_3$) δ ppm: 8.21 (d, 1H, J=1.5 Hz), 8.20 (d, 1H, *J*=1.5 Hz), 8.06 (t, 1H, J= 15 Hz), 7.89 (d, 1H, J=7.5Hz), 7.80 (t, 1H, J=14 Hz), 7.7 (d, 1H, *J*=1.75 Hz), 7.58 (t, 2H, J=7.5 Hz). ^{13}C NMR 125 MHz ($CDCl_3$) δ (ppm): 189.8, 156.3, 149.2, 143.0, 142.5, 141.4, 136.8, 136.6, 132.5, 132.4, 131.5, 130.3, 124.7, 122.5, and 111.5. Mass analysis: m/z=232.0 (**Fig S1**).

Scheme S2. Synthesis of 7-nitro-11H-indeno[1,2-b] quinoxalin-11-one (NIQ) **[1].**

-dihydroxy-1*H*-ne-1,3(2*H*)-dione	4-nitrobenzene-1,2-diamine	7-nitro-11*H*-indeno[1,2-*b*] quinoxalin-11-one

Table S2. Synthesis of NIQ (Scheme S2) **[1]**.

Chemical Name	Mol. wt. (g)	mmol	Quantity(g)	Equivalent
4-nitrophenylene-1,2-diamine	153.1	11	1.7	1.1 eq
Ninhydrin	178.1	10	1.8	1.0 eq
Acetic acid	60.0		10.0 mL	
Methanol			30.0 mL	

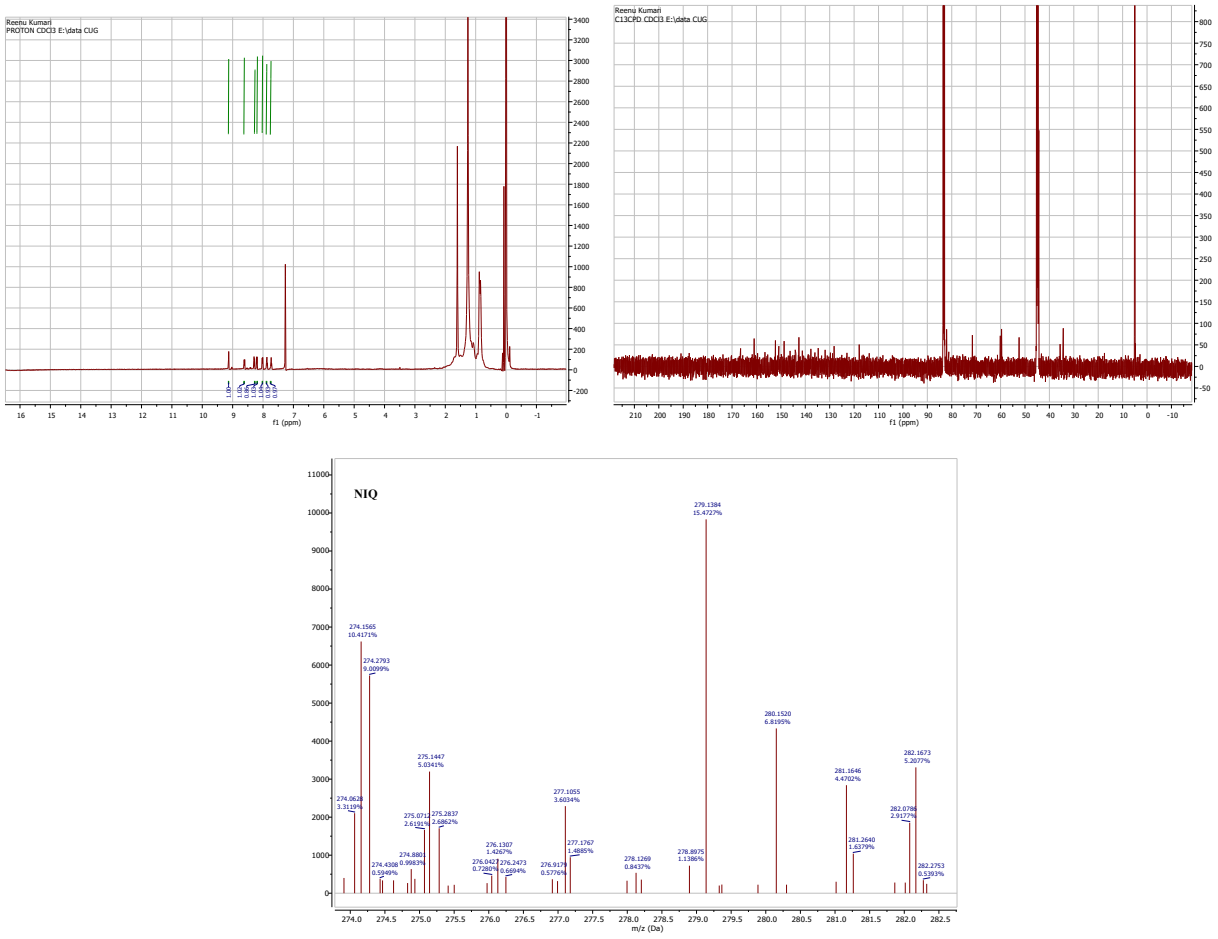

Fig S2. ^{1}H, ^{13}C NMR from our previously reported NIQ study **[1]** validated with mass spectra.

Pale yellow powder yield: 97%, ^{1}H NMR 500 MHz ($CDCl_3$) δ ppm: Aromatic protons 9.13 (s, 1H), 8.61 (d, 1H, *J*=9.46 Hz), 8.29 (d, 1H, *J*=9.00 Hz), 8.20 (d, 1H, *J*=7.50 Hz), 8.02 (d, 1H, *J*=7.41 Hz), 7.87 (t, 1H, J=7.28 Hz), 7.73 (t, 1H, *J*=7.41 Hz). **^{13}C NMR** 125 MHz ($CDCl_3$) δ (ppm): 156.2, 145.1, 145.9, 139.8, 136.4, 134, 130.9, 129.2, 128.2, 125.2, 124.5, 123.8, 123.7, and 77.2. Mass analysis: m/z= 277.1 (**Fig S2**).

Scheme S3. Synthesis of 7-chloro-11H-indeno[1,2-b] quinoxalin-11-one (CIQ)**.**

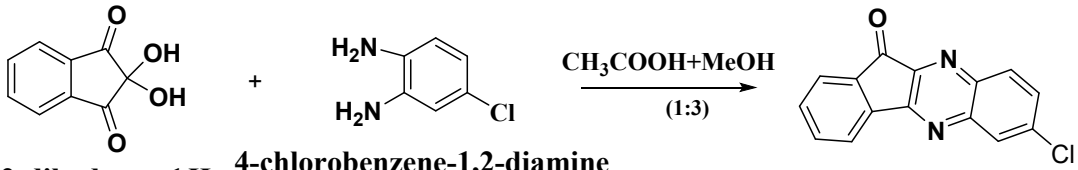

2,2-dihydroxy-1*H*-indene-1,3(2*H*)-dione **4-chlorobenzene-1,2-diamine** **7-chloro-11*H*-indeno[1,2-*b*]quinoxalin-11-one**

Table S3. Synthesis of CIQ (Scheme S3).

Chemical Name	Mol. wt. (g)	mmol	Quantity(g)	Equivalent
4-nitrophenylene-1,2-diamine	142.6	11	1.5	1.1 eq
Ninhydrin	178.1	10	1.8	1.0 eq
Acetic acid	60.0		10.0 mL	
Methanol			30.0 mL	

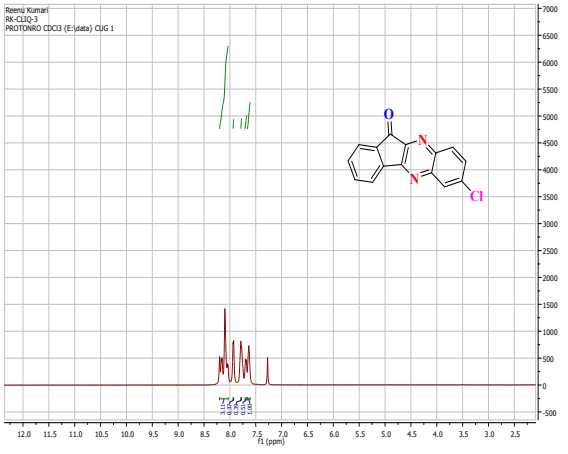

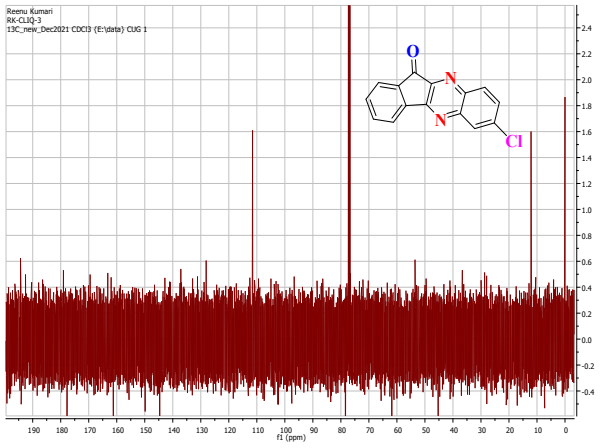

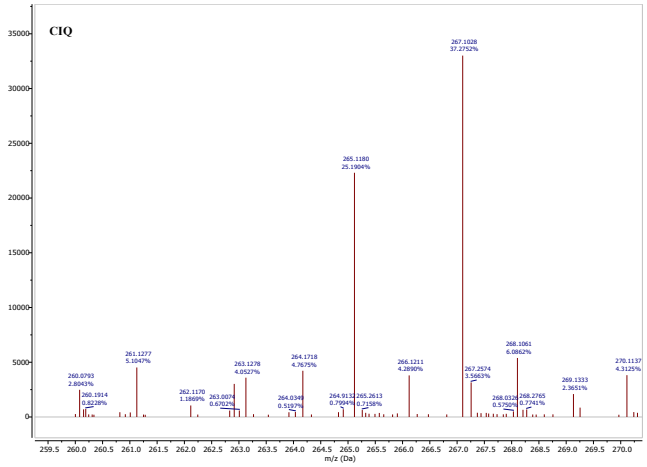

Fig S3. ^{1}H, ^{13}C NMR, and mass spectra for CIQ.

Pale-yellow powder yield (87%) is analyzed with **^{1}H NMR 500 MHz ($CDCl_3$) δ ppm**: 7.62 (s, 1H), 7.68 (d, 1H, J=12.5 Hz), and aromatic protons: 7.78-8.20 (m, 5H). ^{13}C NMR 125 MHz ($CDCl_3$) δ (ppm): 194.3, 178.7, 163.1, 146.2, 142.8, 137.4, 137.1, 132.9, 131.1, 128.0, 112.5, 111.5, 110.8, 110.6, and 109.4. Mass analysis: m/z=266.1 (Fig S3) **[3].**

General procedures for the preparation of starting material:

Scheme S4. The 4-nitrobenzaldehyde (100 mmol, 1.0 eq, 6.6 mL) (Table S4) with LiBr (catalytic amount) in DMF were separately taken in RB and stirred for 1h at RT**.** The reaction was monitored with TLC, product was filtered and dried under vacuum. Structure was analyzed with ^{1}H NMR.

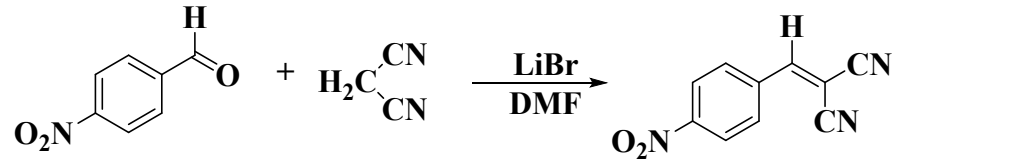

4-nitrobenzaldehyde **malononitrile** **2-(4-nitrobenzylidene)malononitrile**

Table S4. 2-(4-nitrobenzylidene)malononitrile (Scheme S4).

Chemical Name	Mol. wt.(g)	mmol	Quantity(g)	Equivalent
Malononitrile	66.0	100.0	6.6	1.0 eq
4-nitrobenzaldehyde	151.121	100.0	15.1 mL	1.0 eq
Lithium bromide	86.8	100.0	-	1.0 eq
DMF solvent			10.0 mL	

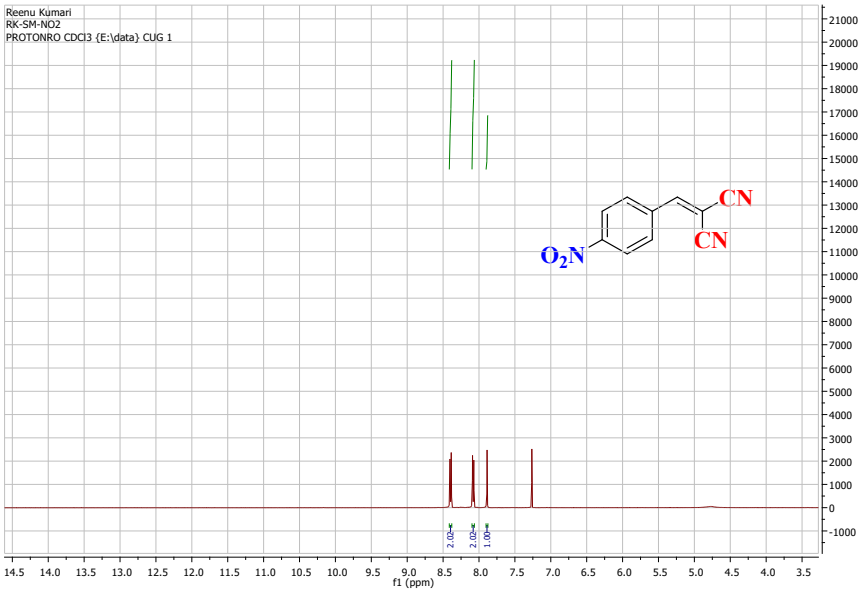

Fig S4. Pale light-yellow powder yield (94%) is analyzed with ^{1}H NMR 500 MHz ($CDCl_3$) δ (ppm): 8.39 (d, 2H, *J*=8.5 Hz), 8.08 (d, 2H, J=8.5 Hz), 7.88 (s, 1H).

Synthesis of SIQPNO$_2$

Scheme S5. Synthesis of 7-nitro-2'-(4-nitrophenyl)-5',6',7',7a'-tetrahydrospiro[indeno[1,2-b]quinoxaline-11,3'-pyrrolizine]-1',1'(2'H)-dicarbonitrile (SIQPNO$_2$).

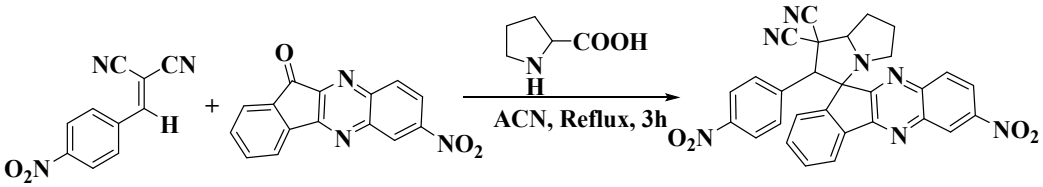

Table S5. Synthesis of SIQPNO$_2$ **(Scheme S5).**

Chemicals	Mol. wt.(g)	mmol	Quantity(g)	Equivalent
2-(4-nitrobenzylidene)malononitrile	154.5	1.0	154.5	1.0 eq
NIQ	277.0	1.0	277.0	1.0 eq
L-proline	115.0	1.0	126.5	1.0 eq
Acetonitrile			15.0 mL	~8.0 eq

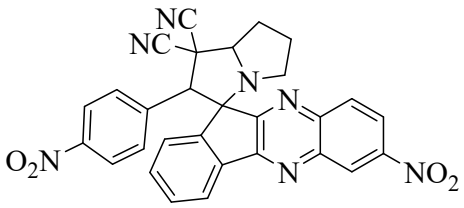

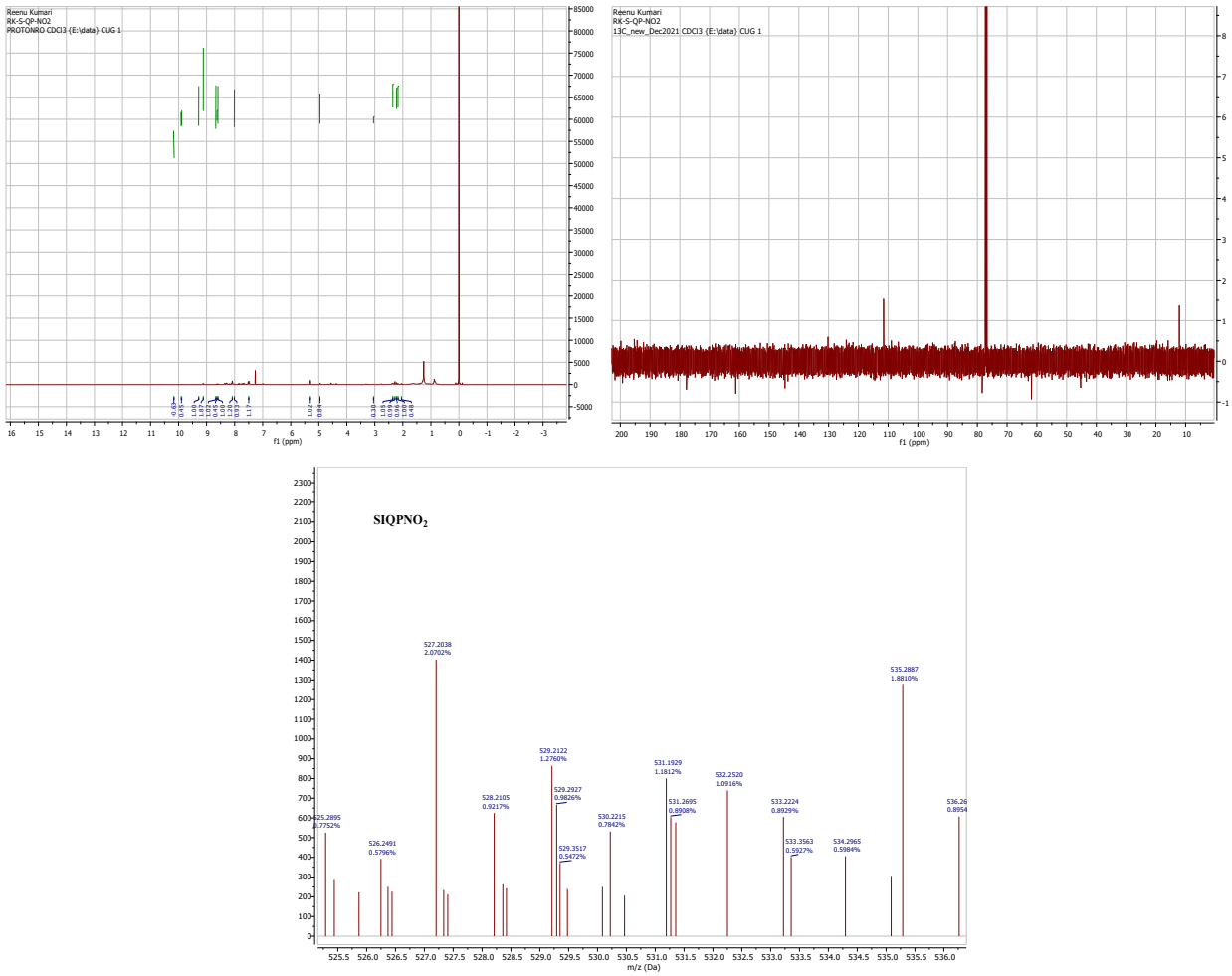

Fig S5 (a-c). ^{1}H, ^{13}C NMR, and mass analysis of $SIQPNO_2$.

Light yellow solid yield (89%) is analyzed with **^{1}H NMR 500 MHz ($CDCl_3$) δ ppm**: Aromatic protons 10.16 (s, 1H), 9.90 (d, 1H, *J*=10 Hz), 9.28 (d, 1H, *J*=4.5 Hz), 9.117 (d, 2H, *J*=3.5 Hz), 8.67 (d, 1H, *J*=2.5 Hz), 8.62 (d, 1H, *J*=2.5 Hz), 8.59 (d, 1H, *J*=2.5 Hz), 8.08 (m, 1H), 8.01 (d, 1H, *J*=7 Hz), 7.49 (m, 1H), 5.3(s, 1H), 4.95 (d, 1H, *J*=5.5 Hz), 2.04-3.04 (m, 6H, $3CH_2$) (Fig S5a). ^{13}C NMR 125 MHz ($CDCl_3$) δ ppm: 168.0, 152.9, 150.5, 144.7, 143.6, 143.6, 138.6, 137.6, 136.1, 130.9, 130.21, 130.20, 128.1, 128.05, 126.9, 124.06, 123.5, 123.16, 121.95, 121.8, 121.7, 111.5, 111.1, 78.7, 61.3, 59.57, 46.57, 27.26, 26.3, 12 (Fig S5b). Mass analysis: m/z=529.2 (Fig S5c).

Scheme S6. A 1:1 ratio of SIQPI+NIQ (**Fig** S6a-b).

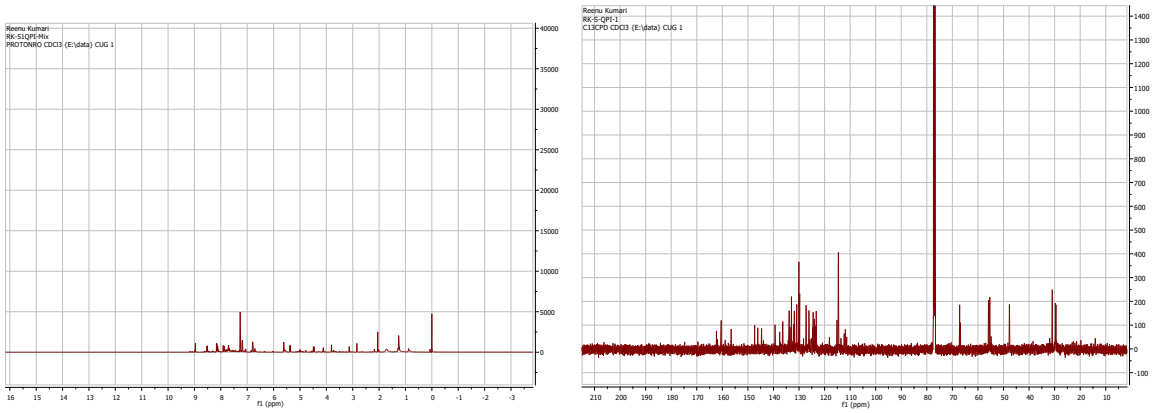

Fig S6a-b. ^{1}H and ^{13}C NMR for Scheme S6 **(125 MHz ($CDCl_3$) δ ppm)**: 160.4, 156.5, 147.4, 146.3, 146.2, 144.3, 139.2, 137.5, 136.3, 133.9, 132.9, 132.1, 131.8, 130.0, 129.7, 127.1, 126.0, 124.0, 123.2, 113.5, 111.9, 111.3, 66.8, 54.9, 47.6, 30.9, 29.7, 29.4, and 14.1.

Scheme S7. 1:1 ratio of SIQPII+NIQ (**Fig S7a-b**).

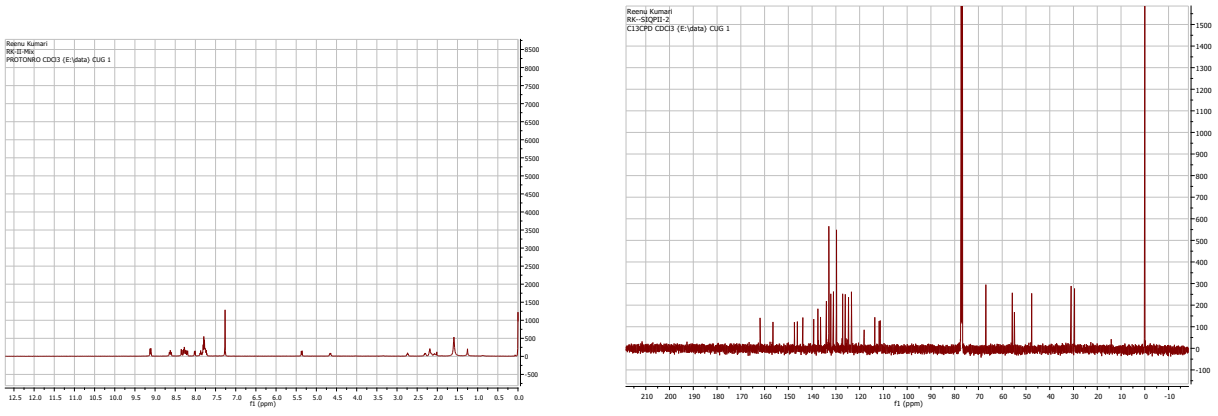

Fig S7a-b.^{1}H and ^{13}C NMR for Scheme S7 (125 MHz ($CDCl_3$) δ ppm): 161.9, 157.7, 156.4, 147.4, 146.2, 143.9, 139.3, 137.5, 136.4, 133.9, 132.9, 132.1, 131.0, 130.9, 129.7, 127.1, 126.0, 124.6, 123.4, 118.1, 113.6, 111.7, 111.3, 66.8, 54.8, 47.6, 30.9, 29.7, 29.5, and 14.1.

Scheme S8. A 1:1 ratio of SIQPIII+NIQ (**Fig S8a-b**).

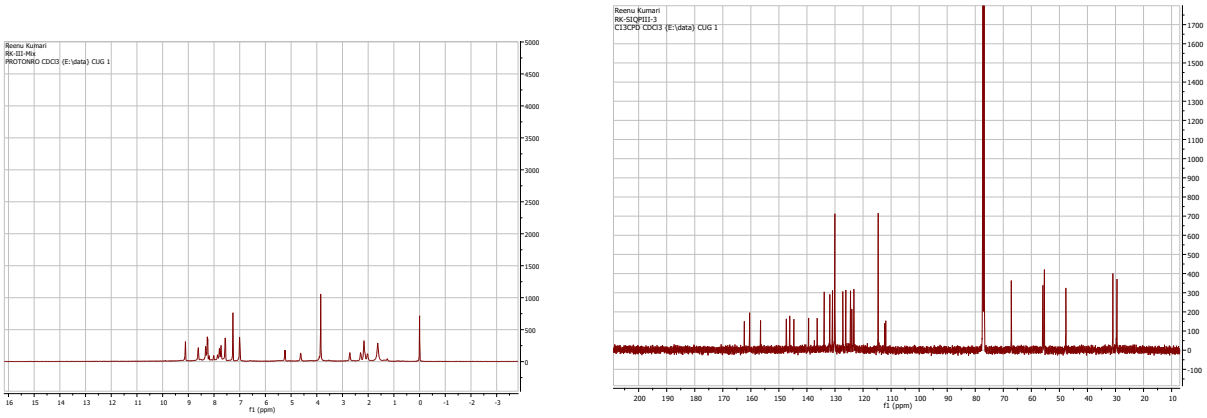

Fig S8a-b. ^{13}C NMR for Scheme S8 (125 MHz ($CDCl_3$) δ ppm): 187.4, 170.7, 162.3, 160.4, 156.5, 147.3, 146.1, 144.6, 139.3, 137.3, 136.3, 133.8, 131.8, 130.8, 130.0, 127.2, 126.1, 124.5, 124.0, 123.2, 114.6, 112.4, 111.8, 67.1, 55.9, 55.5, 55.3, 47.6, 30.9, and 29.4.

Scheme S9. Reaction scope, all reactions could carry out with ninhydrin (10 mmol, 1.0 eq, 1.8 g) and stirred in a solvent mixture of CH_3COOH (10 mL) and CH_3OH (30 mL) 1:3 ratio for 30 min at RT for IQPs**) [1].**

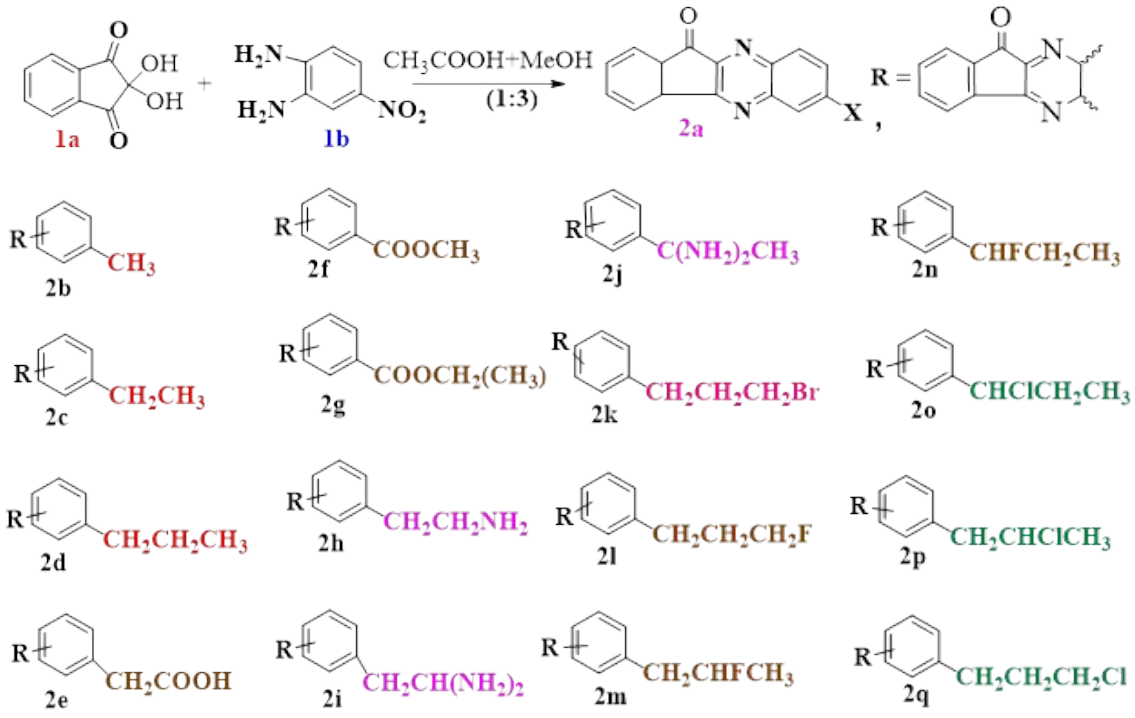

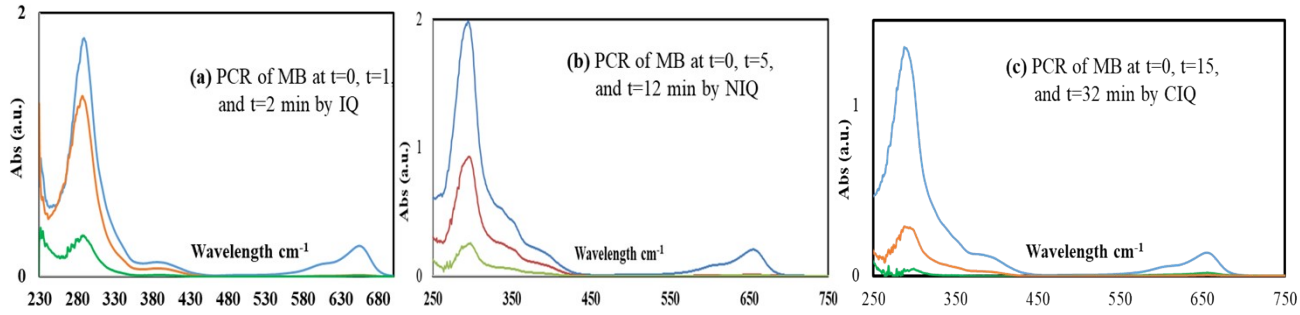

Fig S9. UV-Vis spectra for MB PCR by **(a)** IQ, **(b)** NIQ, and **(c)** CIQ.

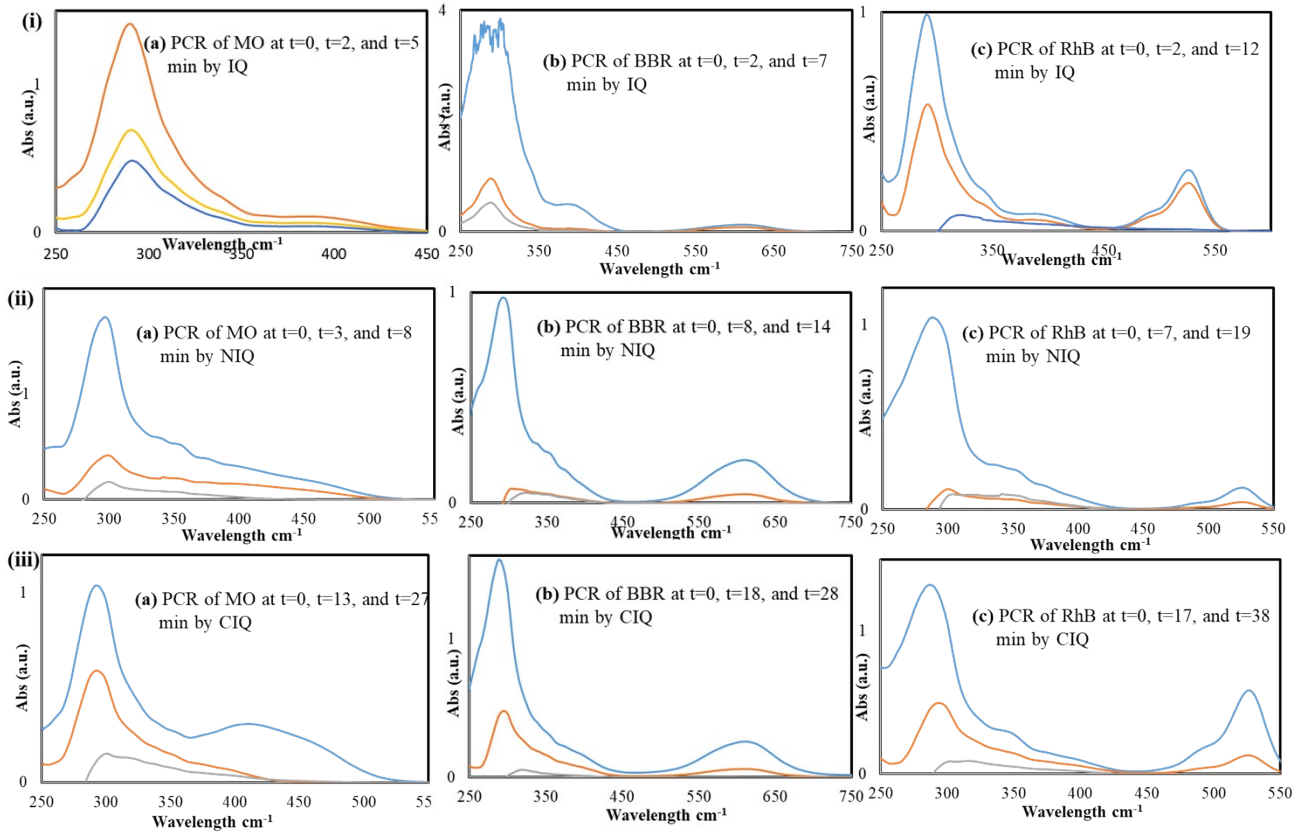

Fig S10. UV-Vis for **(a)** MO, **(b)** BBR, and **(c)** RhB PCR by **(i)** IQ, **(ii)** NIQ, and **(iii)** CIQ.

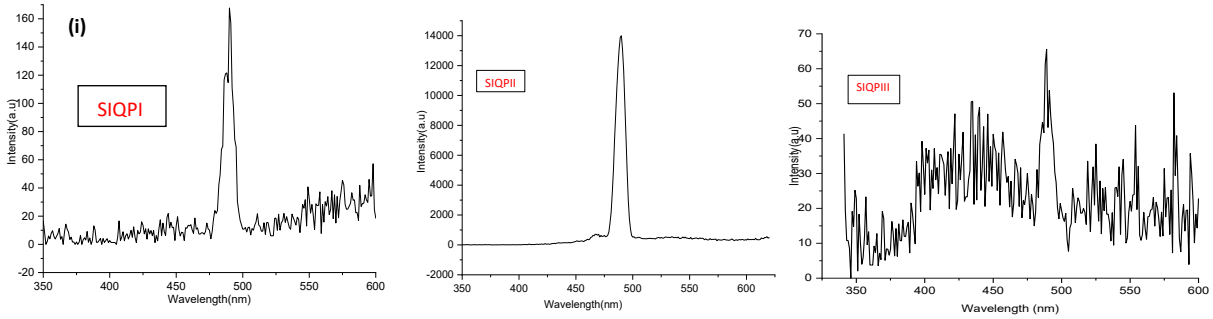

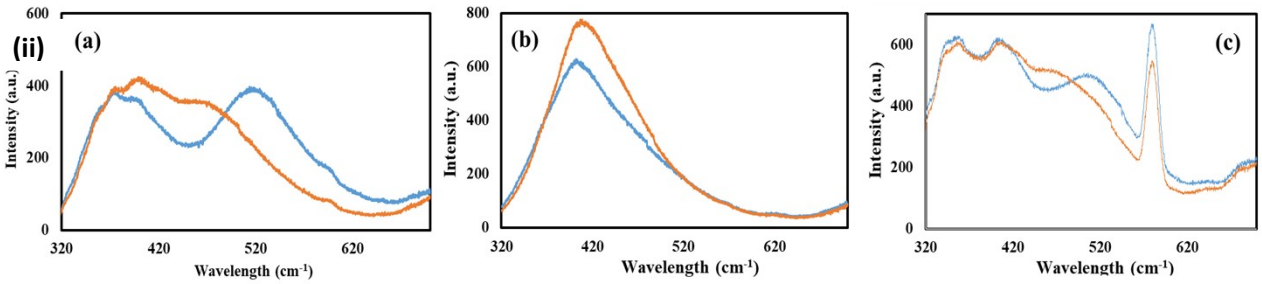

Fig S11. Fluorescence: **(i)** alone SIQPI, II, III (Note: taken from previous study for comparison) **[2] (ii)** before and after MO reduction by **(a)** IQ, **(b)** NIQ, and **(c)** CIQ.

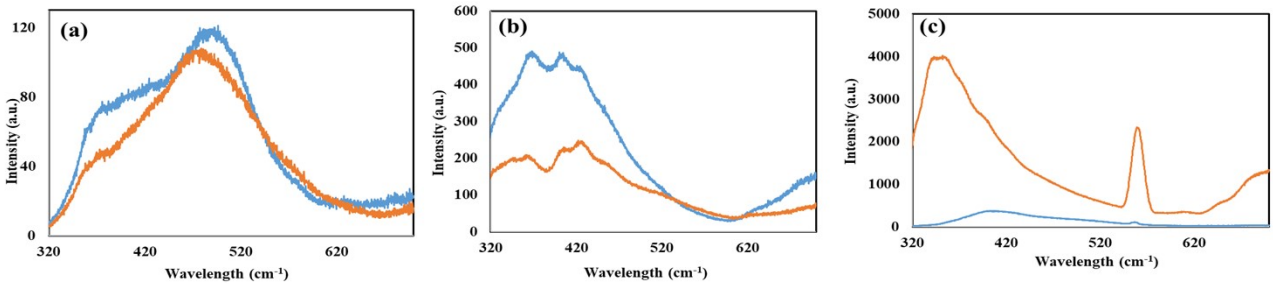

Fig S12. Fluorescence before and after BBR reduction by **(a)** IQ, **(b)** NIQ, and **(c)** CIQ.

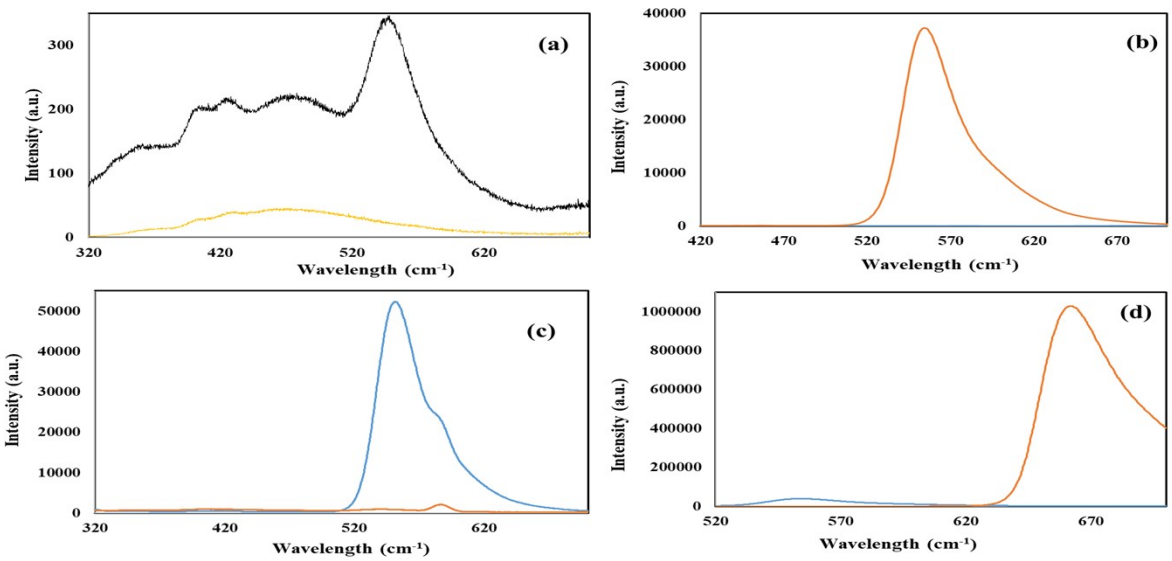

Fig S13. Fluorescence before and after RhB reduction using **(a)** IQ **(b)** NIQ **(c)** CIQ and **(d)** $SIQPNO_2$.

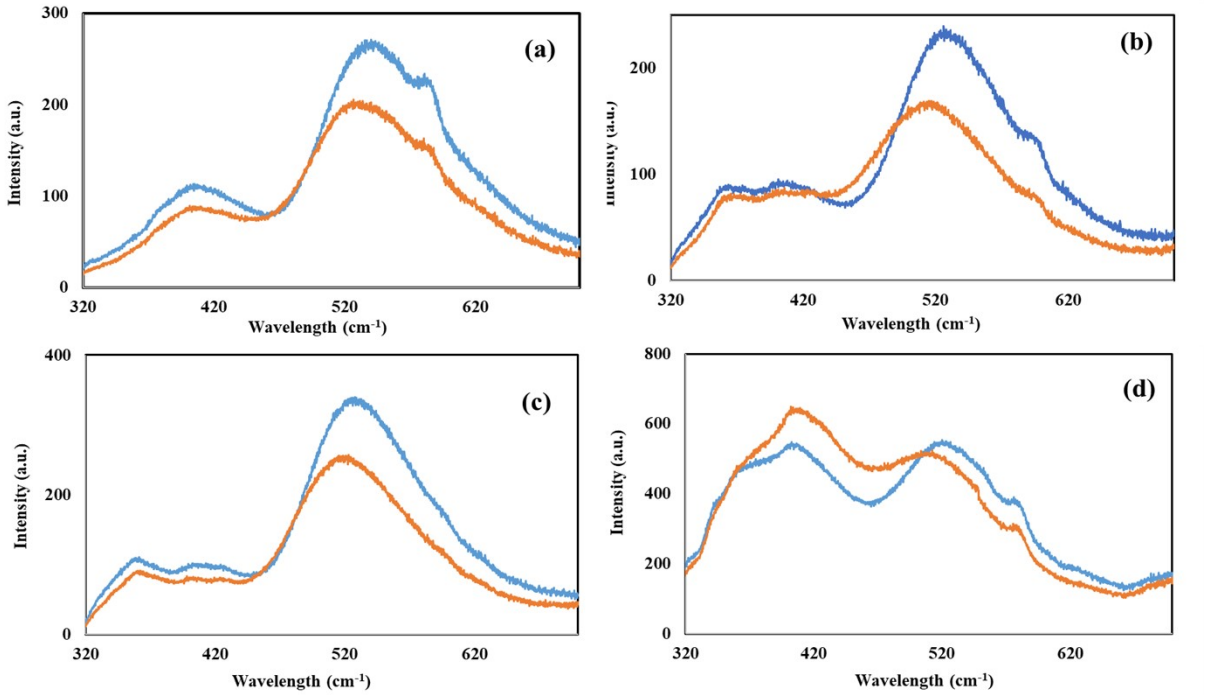

Fig S14. Fluorescence before and after MO reduction using IQ with **(a)** LaGT, **(b)** CeGT, **(c)** TbGT, and **(d)** HoGT.

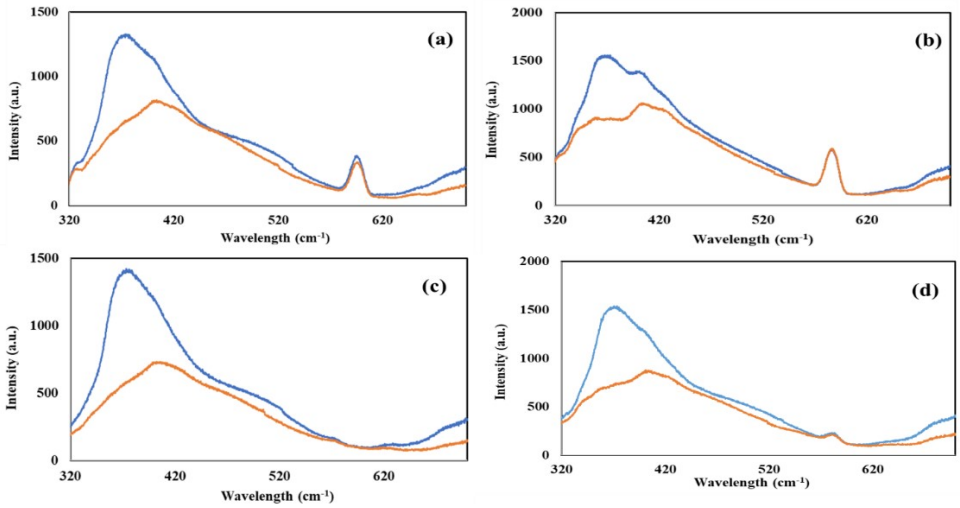

Fig S15. Fluorescence before and after BBR reduction using IQ with **(a)** LaGT, **(b)** CeGT, **(c)** TbGT, and **(d)** HoGT.

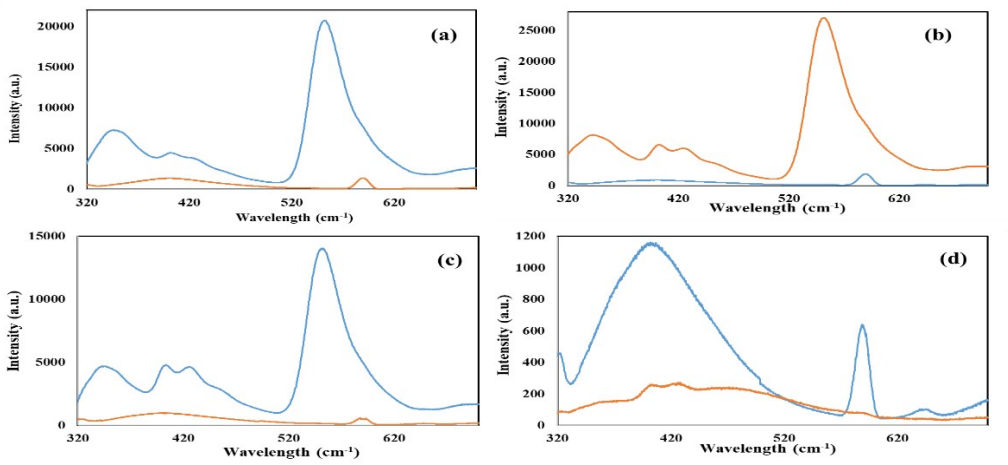

Fig S16. Fluorescence before and after RhB reduction using IQ with **(a)** LaGT, **(b)** CeGT, **(c)** TbGT, and **(d)** HoGT.

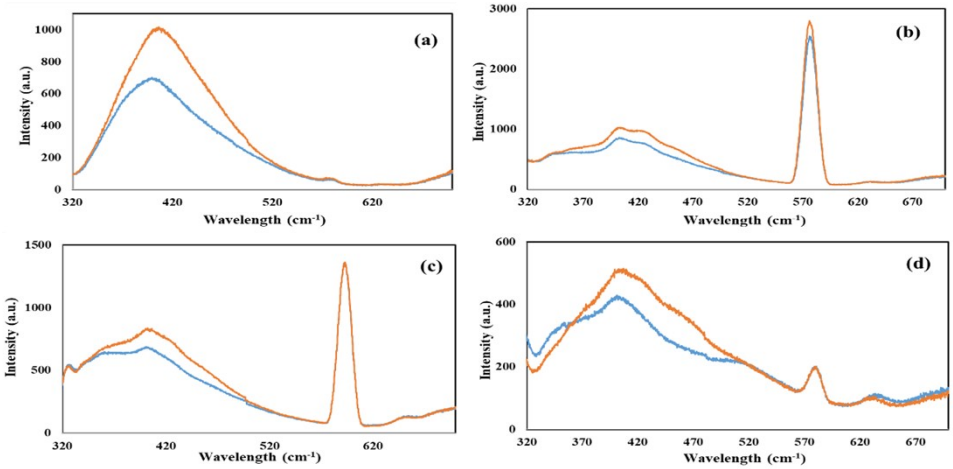

Fig S17. Fluorescence before and after MO reduction using NIQ with **(a)** LaGT, **(b)** CeGT, **(c)** TbGT, and **(d)** HoGT.

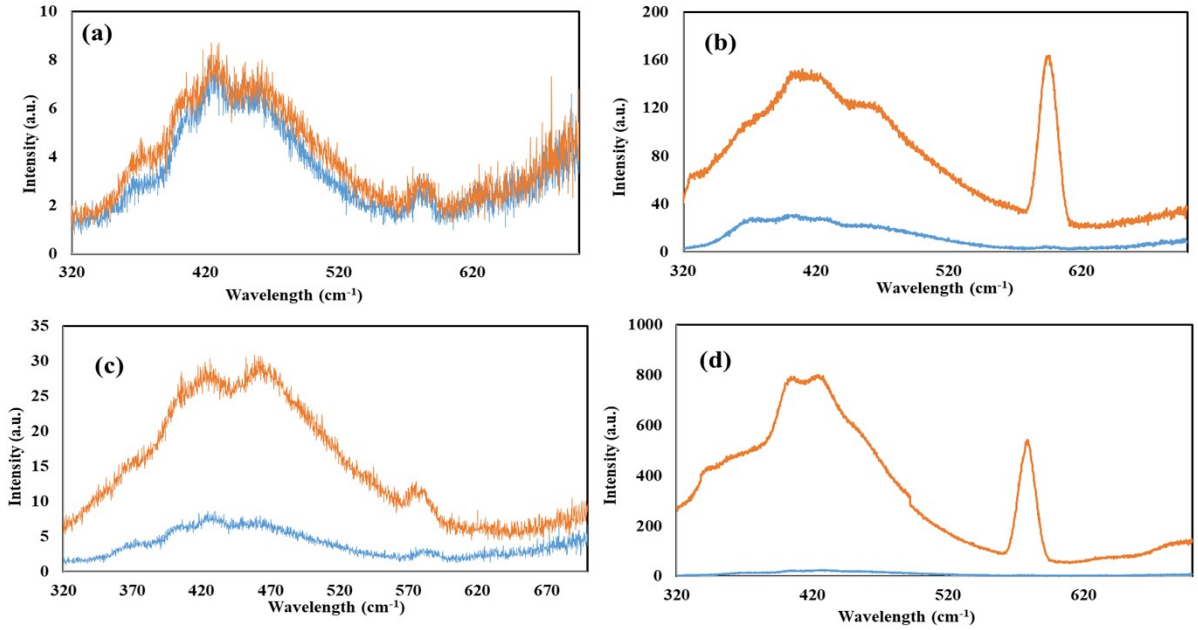

Fig S18. Fluorescence before and after BBR reduction using NIQ with **(a)** LaGT, **(b)** CeGT, **(c)** TbGT, and **(d)** HoGT.

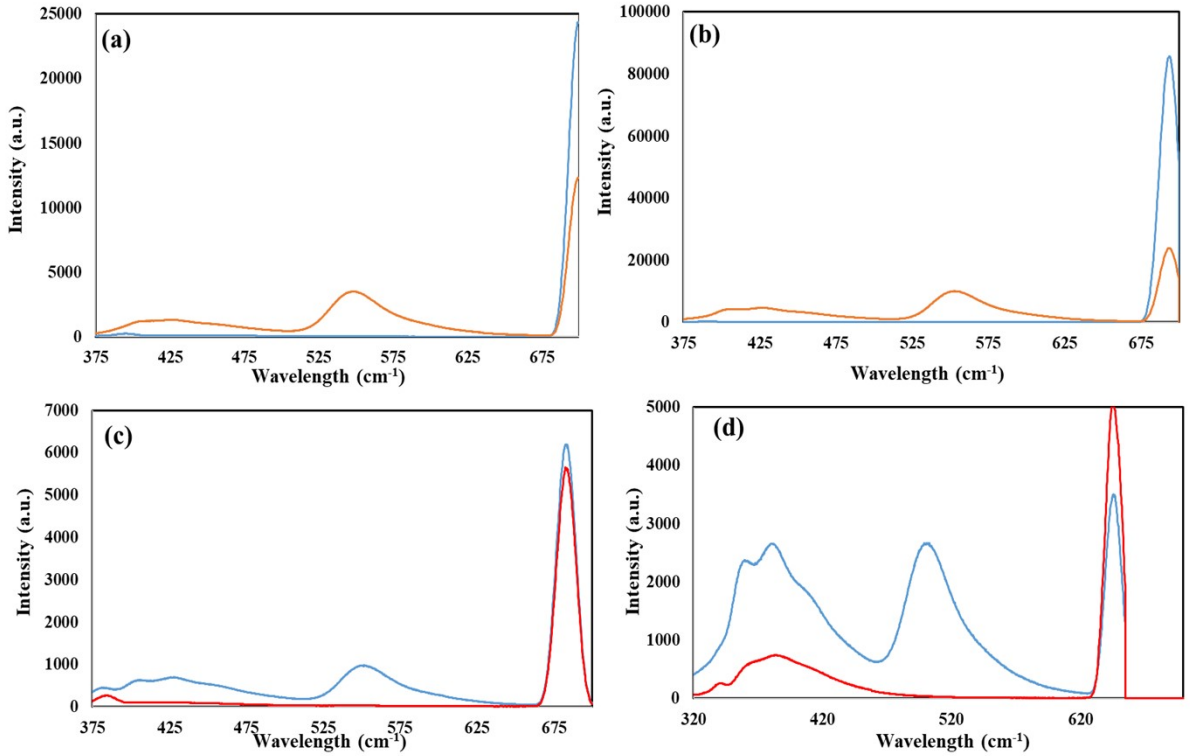

Fig S19. Fluorescence before and after RhB reduction using NIQ with **(a)** LaGT, **(b)** CeGT, **(c)** TbGT, and **(d)** HoGT.

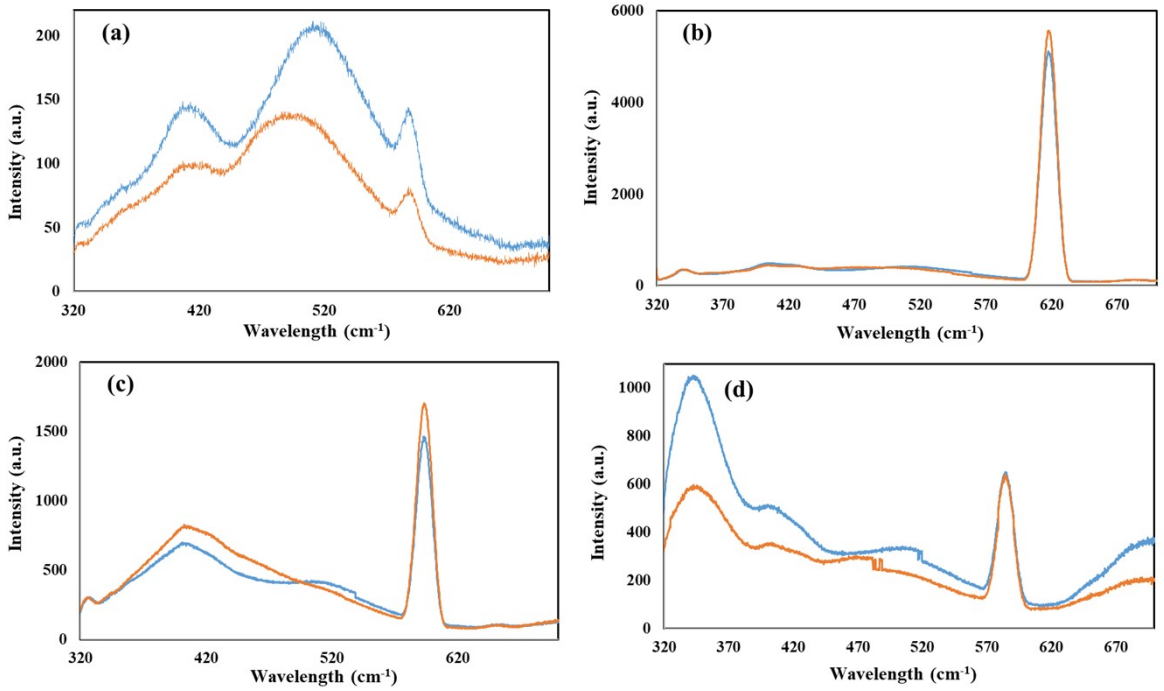

Fig S20. Fluorescence before and after MO reduction using CIQ with **(a)** LaGT, **(b)** CeGT, **(c)** TbGT, and **(d)** HoGT.

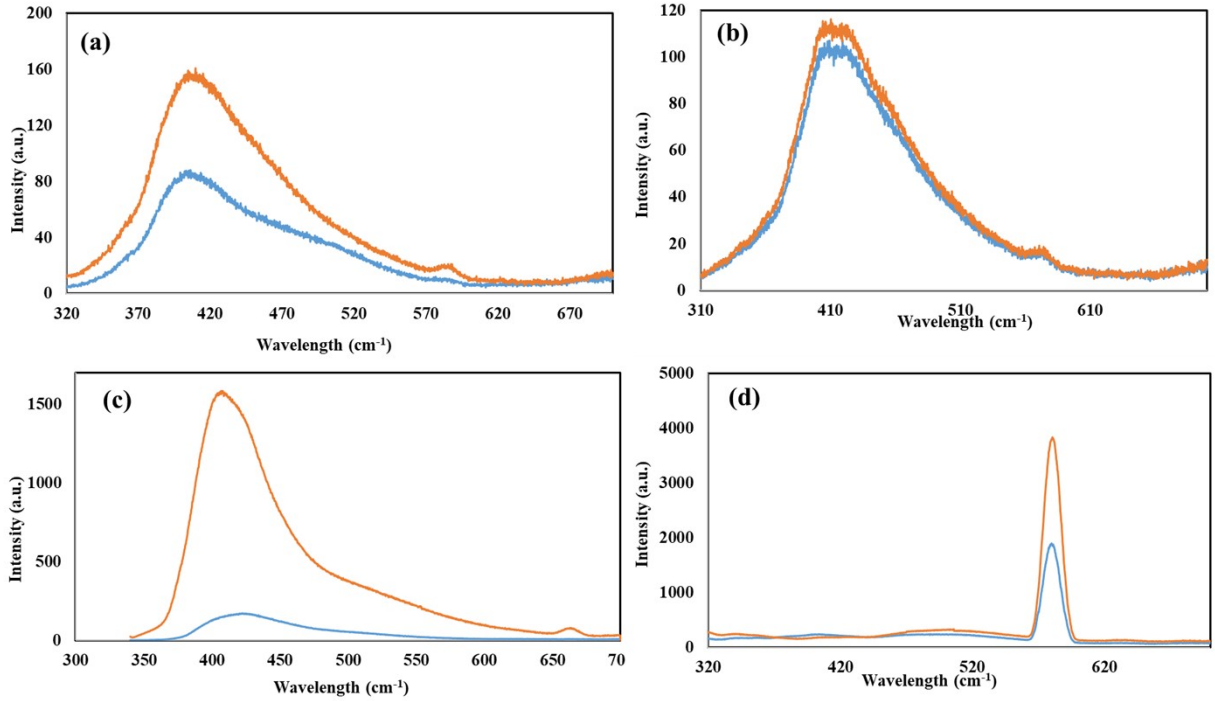

Fig S21. Fluorescence before and after BBR reduction using with CIQ **(a)** LaGT, **(b)** CeGT, **(c)** TbGT, and **(d)** HoGT.

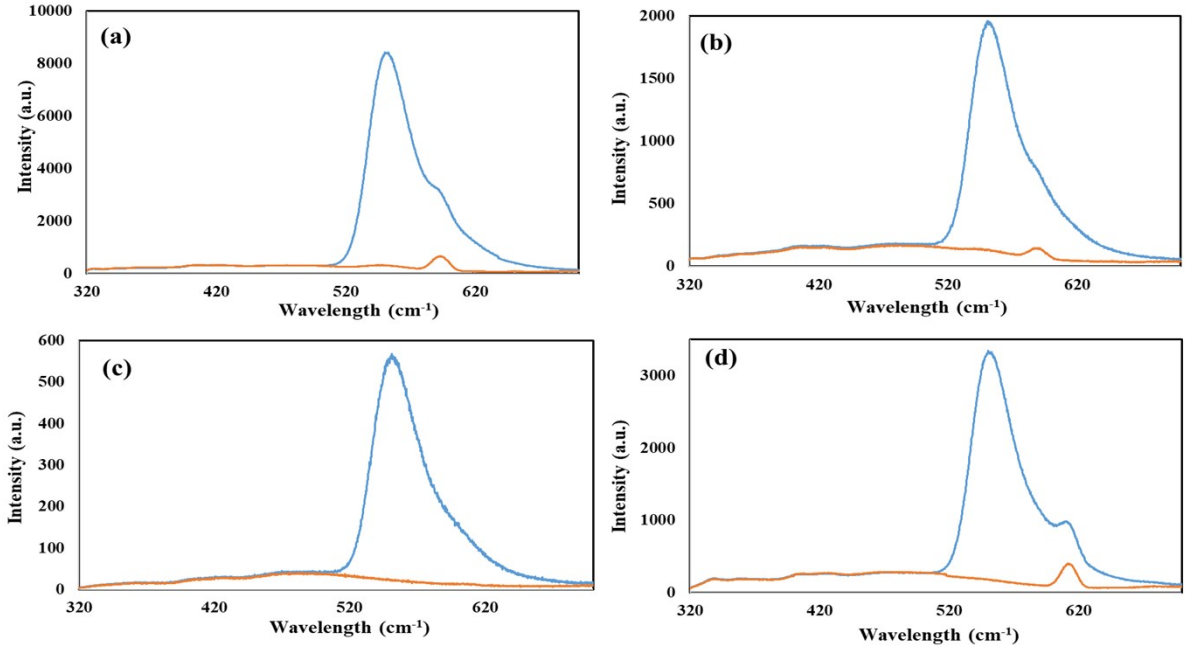

Fig S22. Fluorescence before and after RhB reduction using CIQ with **(a)** LaGT, **(b)** CeGT, **(c)** TbGT, and **(d)** HoGT.

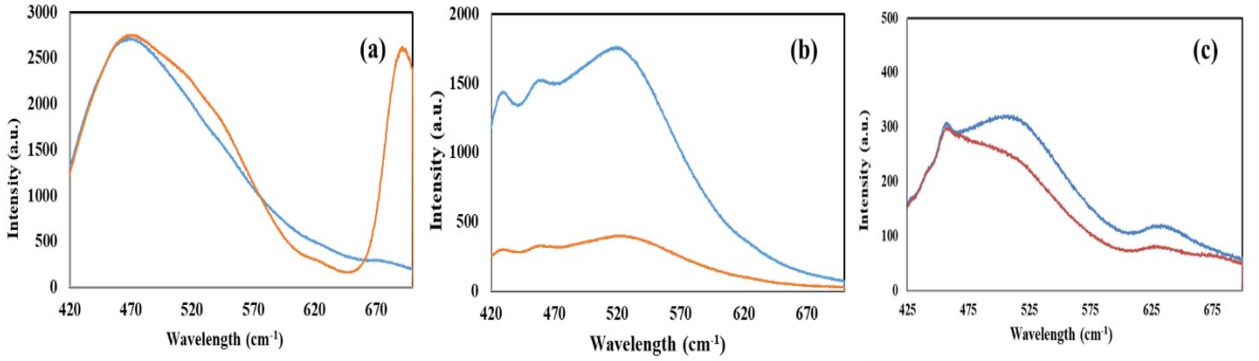

Fig S23. Fluorescence before and after reduction of **(a)** MB, **(b)** MO, and **(c)** BBR by $SIQPNO_2$.

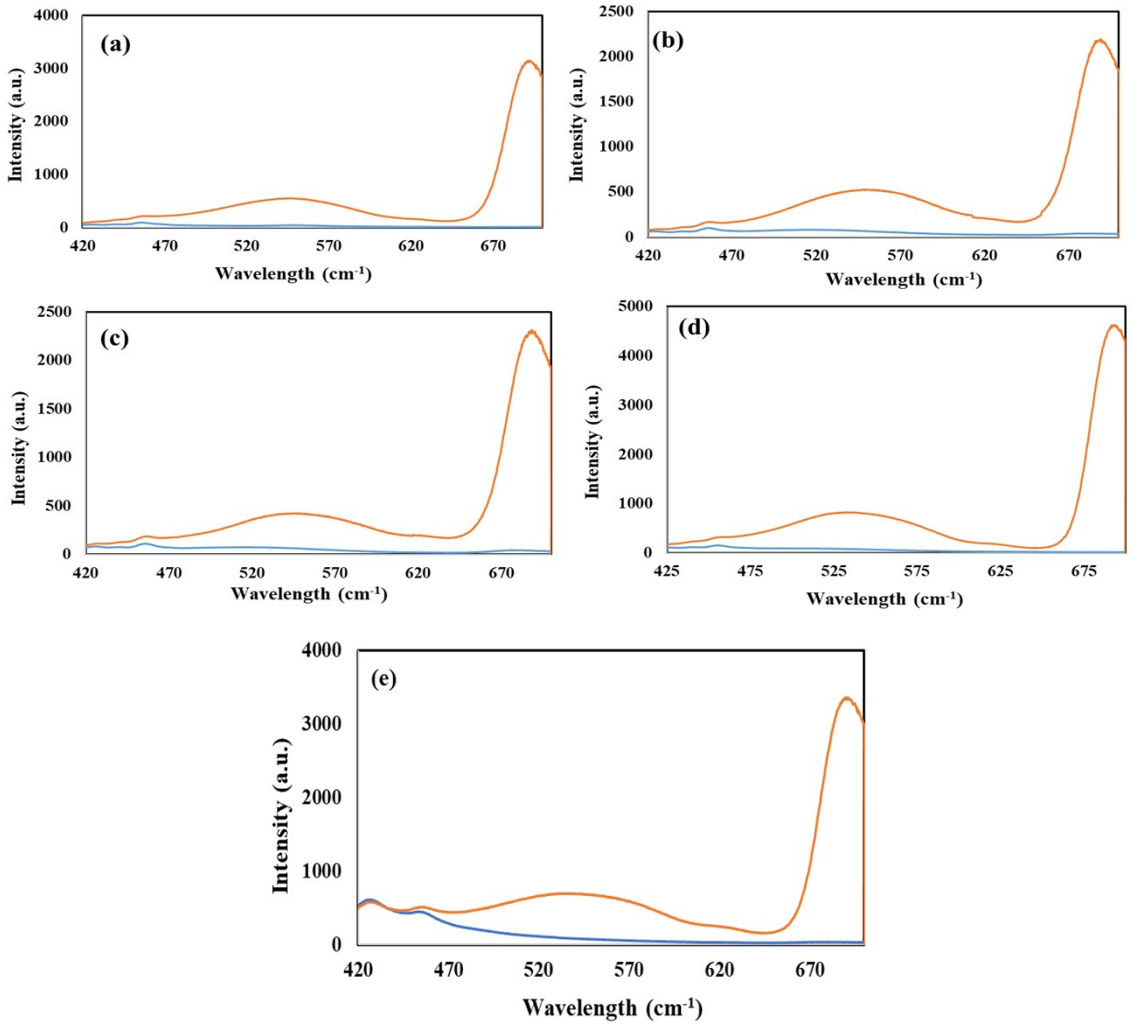

Fig. S24. Fluorescence before and after MB reduction using $SIQPNO_2$ with **(a)** LaGT, **(b)** CeGT, **(c)** TbGT, **(d)** HoGT, and **(e)** NIQ.

Table S6. Comparative study of RhB, BBR, MO, and MB with HoGT, CeGT, TbGT, and LaGT

	HoGT	CeGT	TbGT	LaGT	HoGT	CeGT	TbGT	LaGT	HoGT	CeGT	TbGT	LaGT	HoGT	CeGT	TbGT	LaGT
	RhB PCR time (min)				BBR PCR time (min)				MO PCR time (min)				MB PCR time (min)			
a	86	76	73	55	28	30	25	12	21	25	17	15	13	10	11	7
b	90	78	78	61	33	38	32	25	22	34	16	08	28	31	23	18
c	77	84	68	60	28	33	28	21	16	31	23	18	51	55	45	33
d													197	242	225	88

using (**i**) **a**=IQ, (**ii**) **b**=NIQ, (**iii**) **c**=CIQ, and (**iv**) **d**=$SIQPNO_2$.

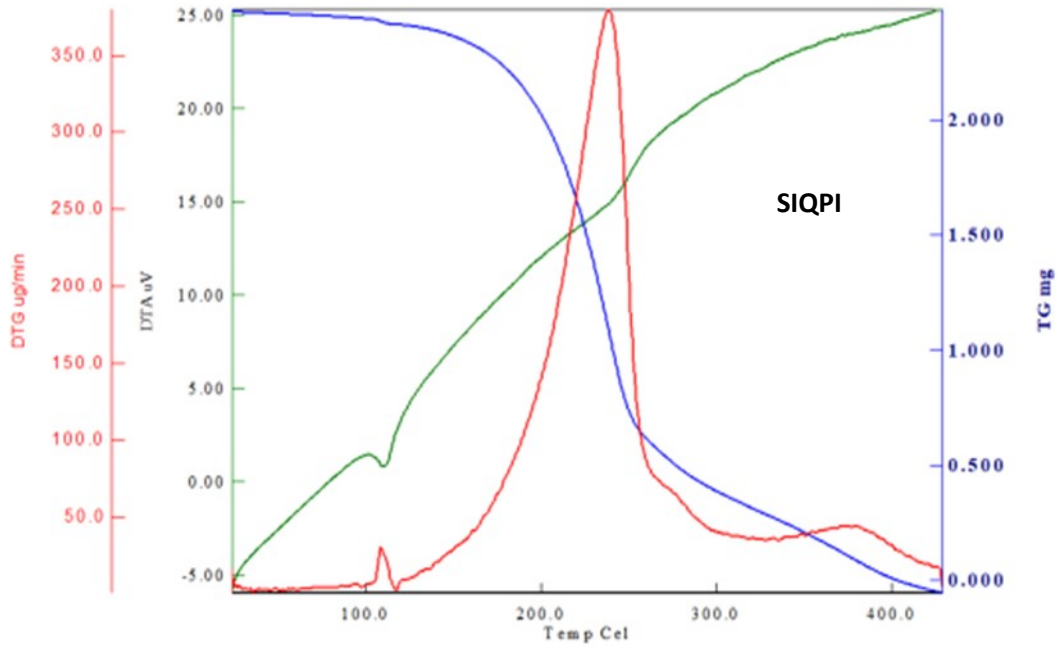
SIQPI
DTG ug/min
DTA uV
TG mg
Temp Cel
350.0
300.0
250.0
200.0
150.0
100.0
50.0
25.00
20.00
15.00
10.00
5.00
0.00
-5.00
2.000
1.500
1.000
0.500
0.000
100.0
200.0
300.0
400.0

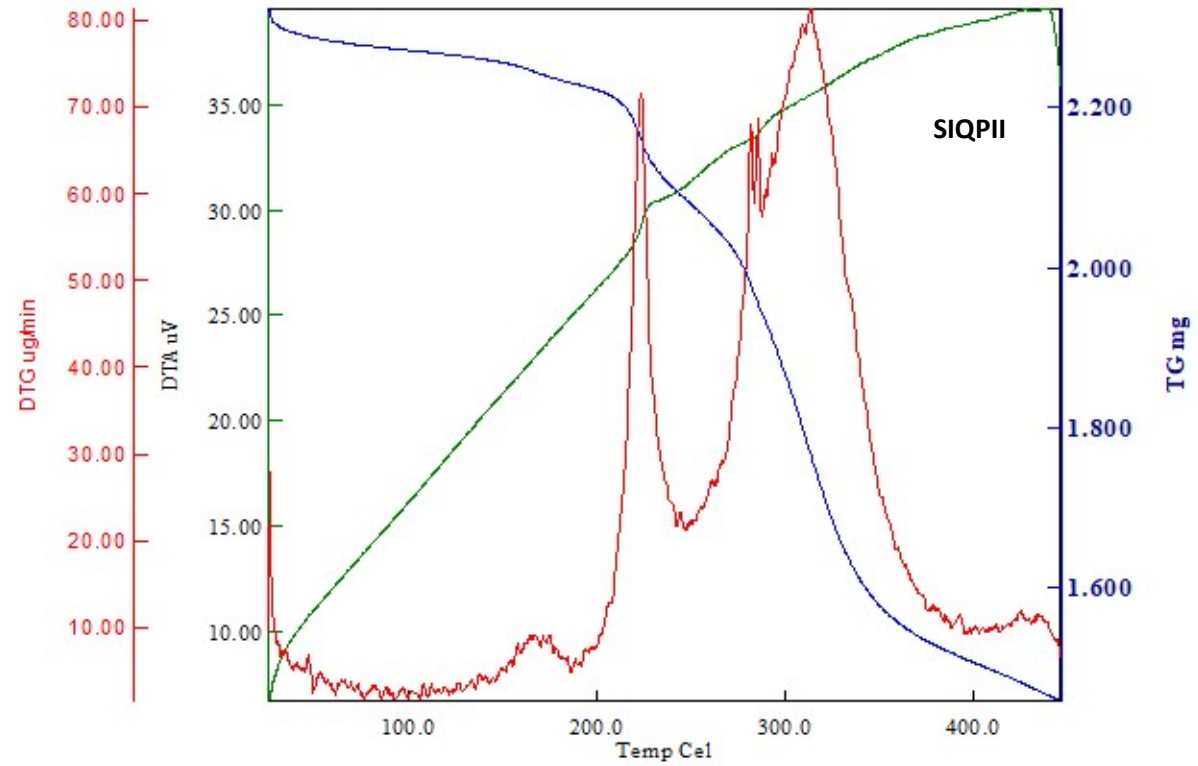
SIQPII
DTG ug/min
DTA uV
TG mg
Temp Cel
80.00
70.00
60.00
50.00
40.00
30.00
20.00
10.00
35.00
30.00
25.00
20.00
15.00
10.00
2.200
2.000
1.800
1.600
100.0
200.0
300.0
400.0

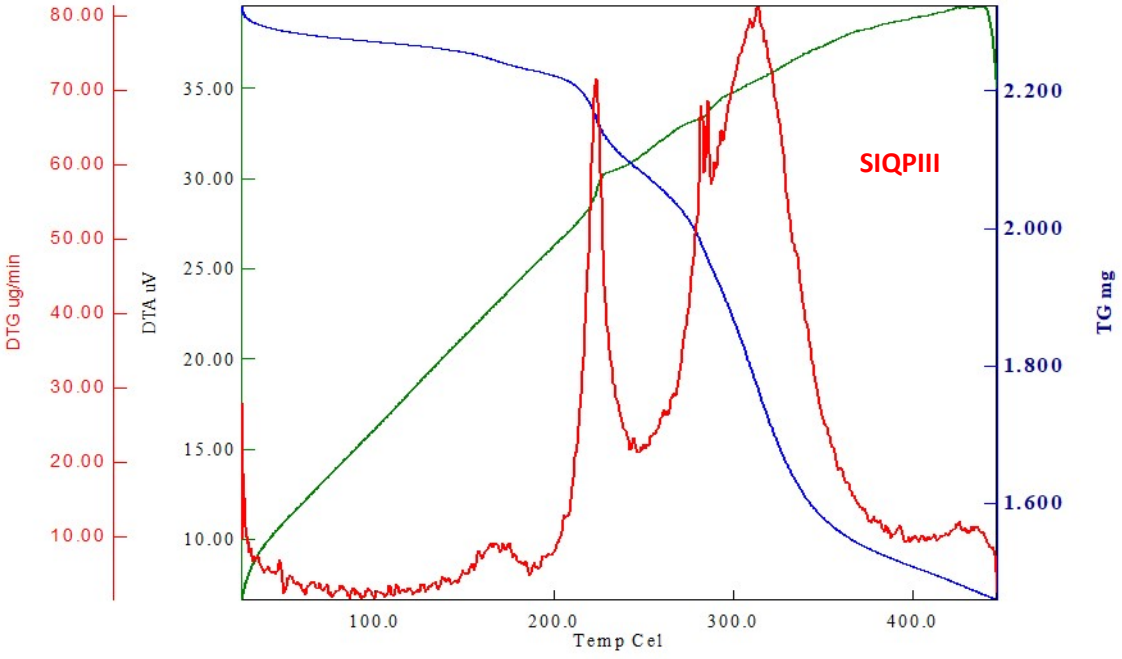
SIQPIII
DTG ug/min
DTA uV
TG mg
Temp Cel
80.00
70.00
60.00
50.00
40.00
30.00
20.00
10.00
35.00
30.00
25.00
20.00
15.00
10.00
2.200
2.000
1.800
1.600
100.0
200.0
300.0
400.0

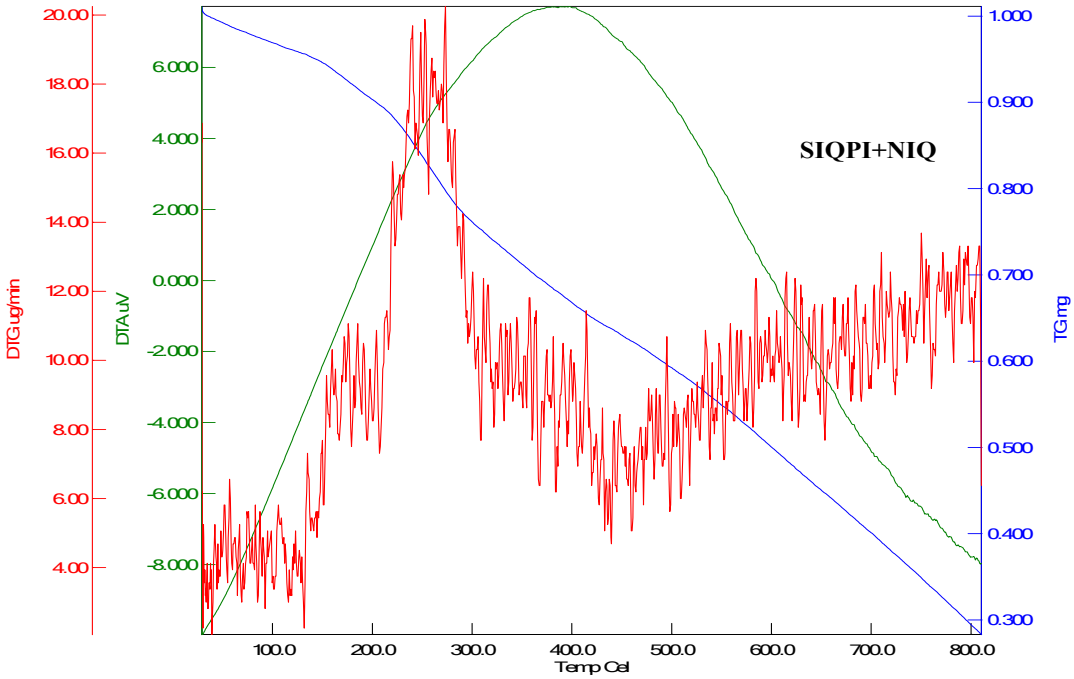
SIQPI+NIQ
DTG ug/min
DTA uV
TG mg
Temp Cel

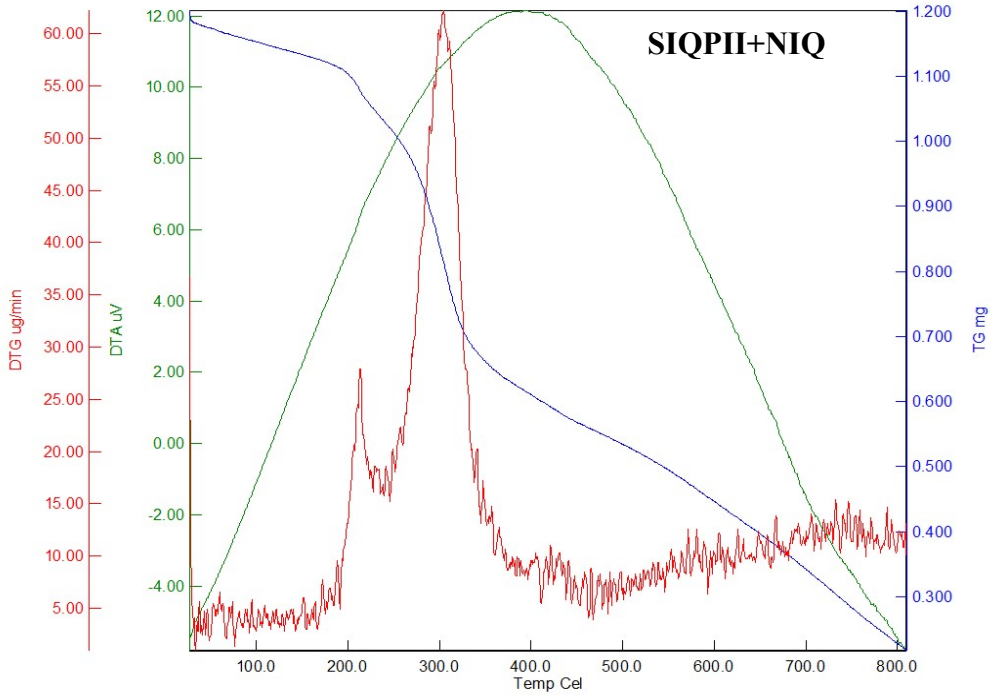
SIQPII+NIQ
DTG ug/min
DTA uV
TG mg
Temp Cel

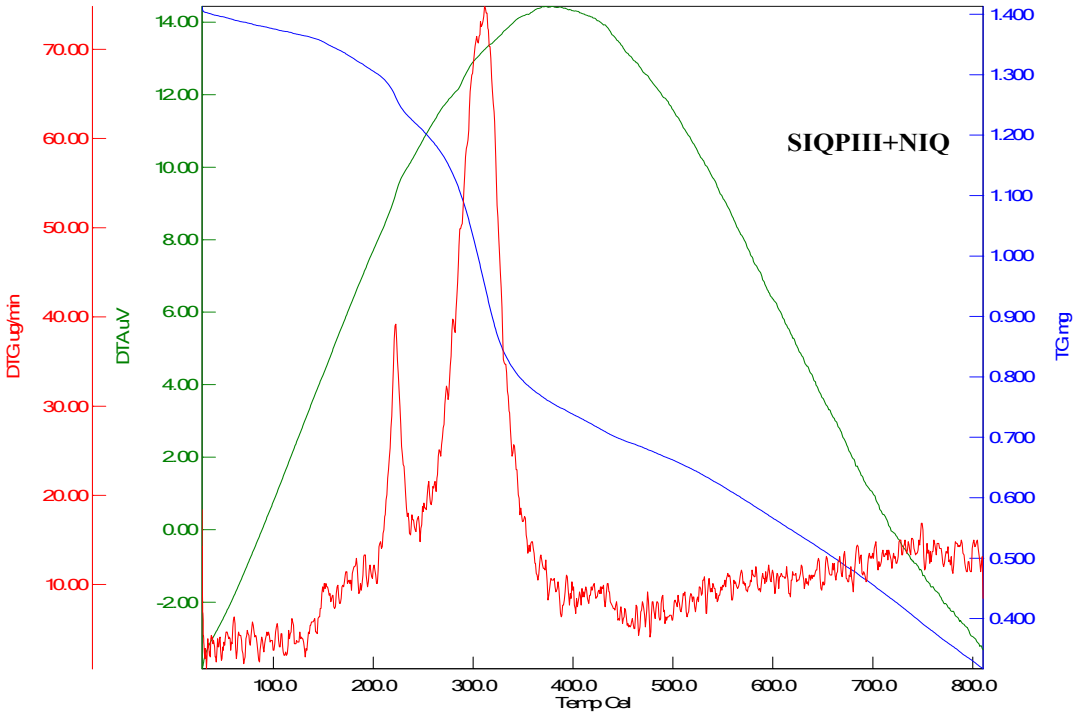

Fig S25. TGA of SIQPI, II, III, (Note: taken from previous study for comparison) **[1]** and SIQPI+NIQ, SIQPII+NIQ, and SIQPIII+NIQ**.**

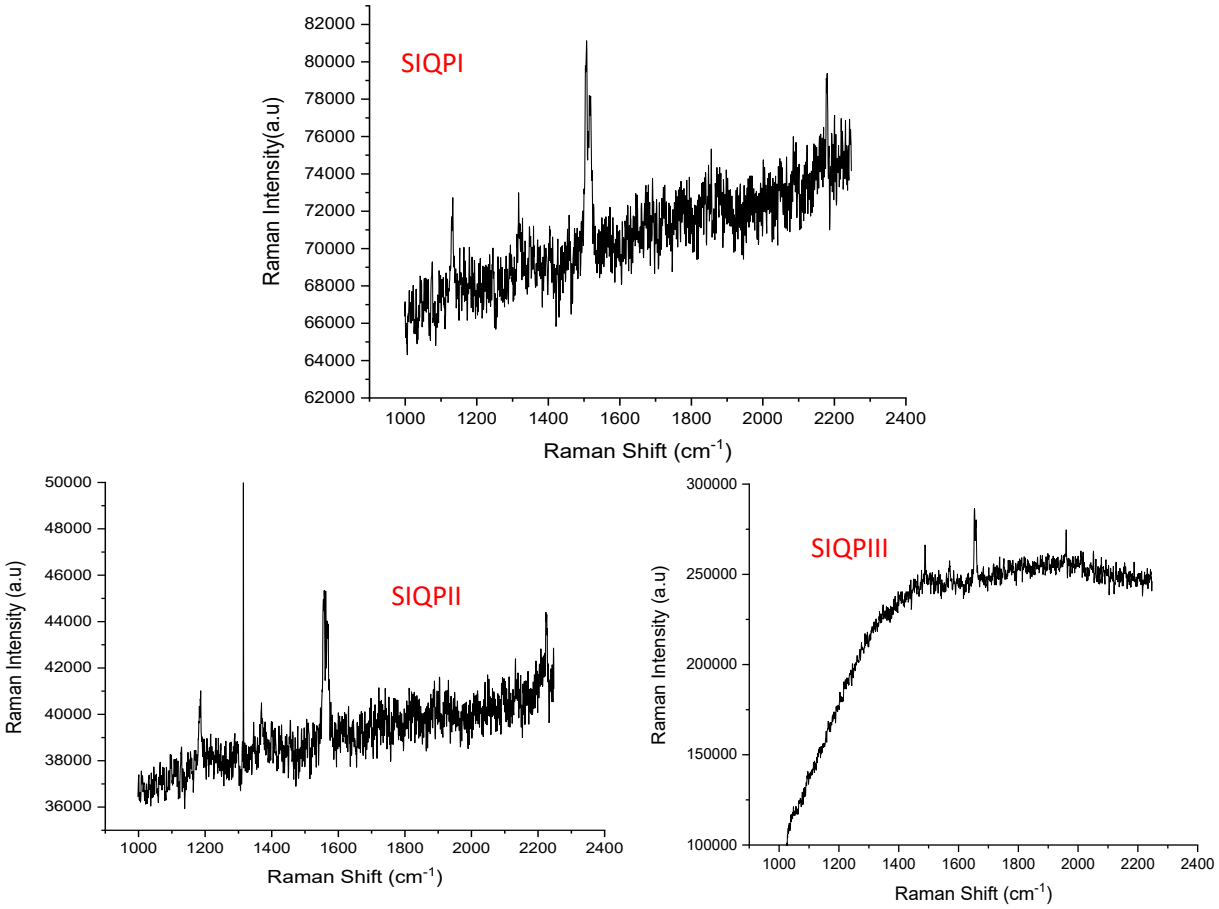

Fig S26 (a). Raman of alone SIQPI, II, and III(Note: taken from previous study for comparison) **[1].**

Table S7. Elemental study for C, N, and H % with IQPs, $SIQPNO_2$, SIQPs+NIQ, and $SIQPNO_2$+NIQ.

Molecules	**N (%)**	**C (%)**	**H (%)**	**S (%)**	**O (%)**	**wt (mg)**
IQ	11.482	75.502	3.318	-	-	1.029
NIQ	14.714	63.039	2.489	-	-	1.047
CIQ	10.509	65.867	2.532	-	-	1.030
$SIQPNO_2$	13.915	66.049	4.627	-	-	1.008
I+NIQ	14.850	62.267	2.449	-	-	1.054
II+NIQ	14.913	62.252	2.487	-	-	1.027
III+NIQ	15.578	63.025	2.668	-	-	1.037
$SIQPNO_2$+NIQ	14.893	62.505	2.529	-	-	1.060

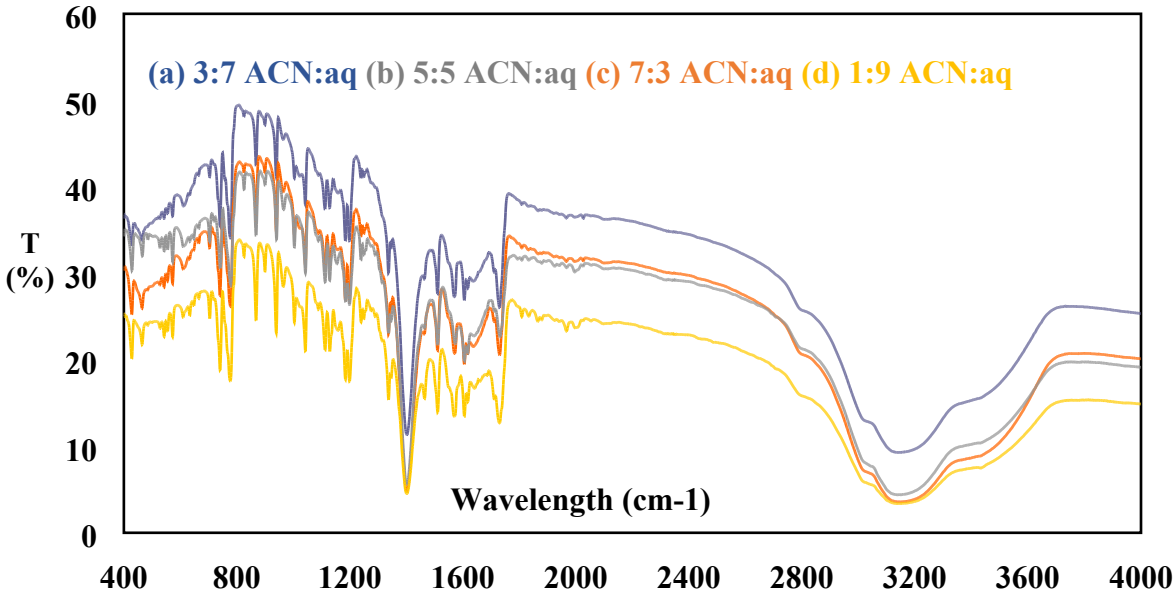

Fig S26 (b). IQ+Fe in **(a)** 3:7, (b) 5:5, **(c)** 7:3, and **(d)** 1:9 of ACN:aq solvent ratios.

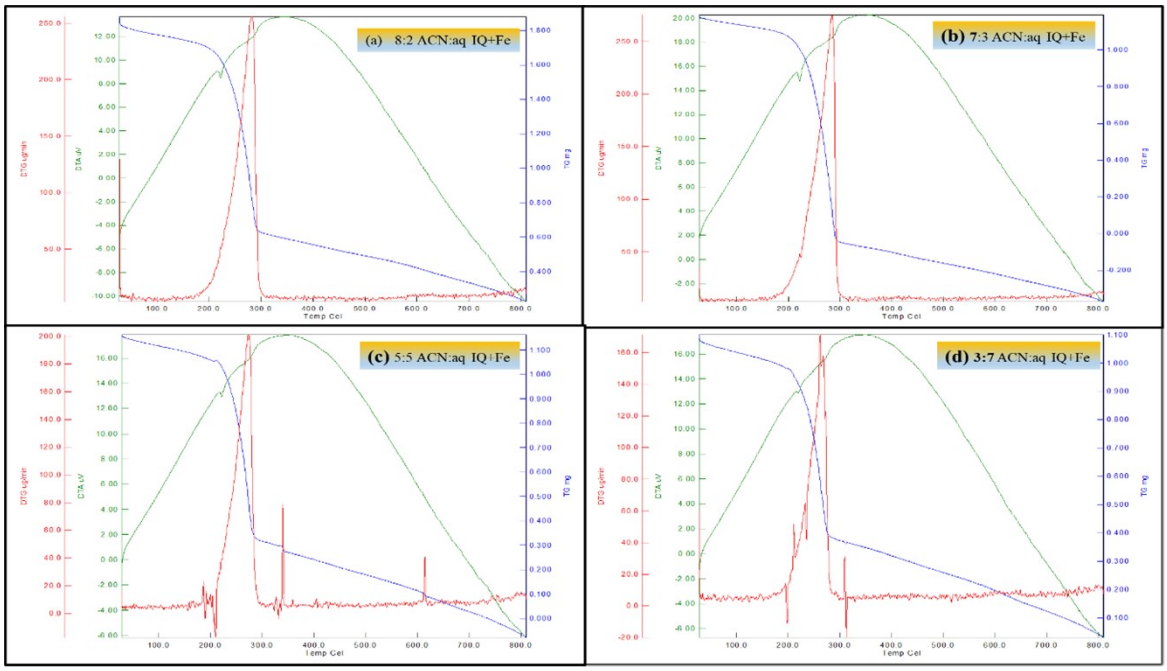

Fig S27. TGA of IQ+Fe in (a) 8:2, (b) 7:3, (c) 5:5, and (d) 3:7 of ACN:aq ratio.

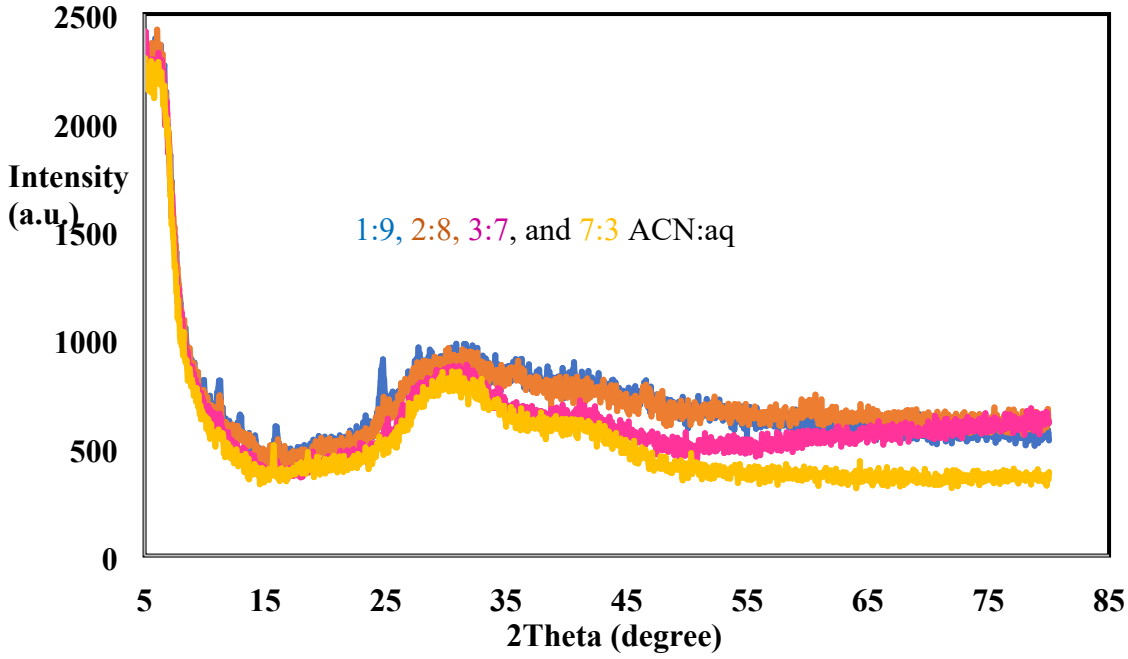

Fig S28. XRD spectra of IQ+Fe in different solvent ratio of ACN:aq after 26 days.

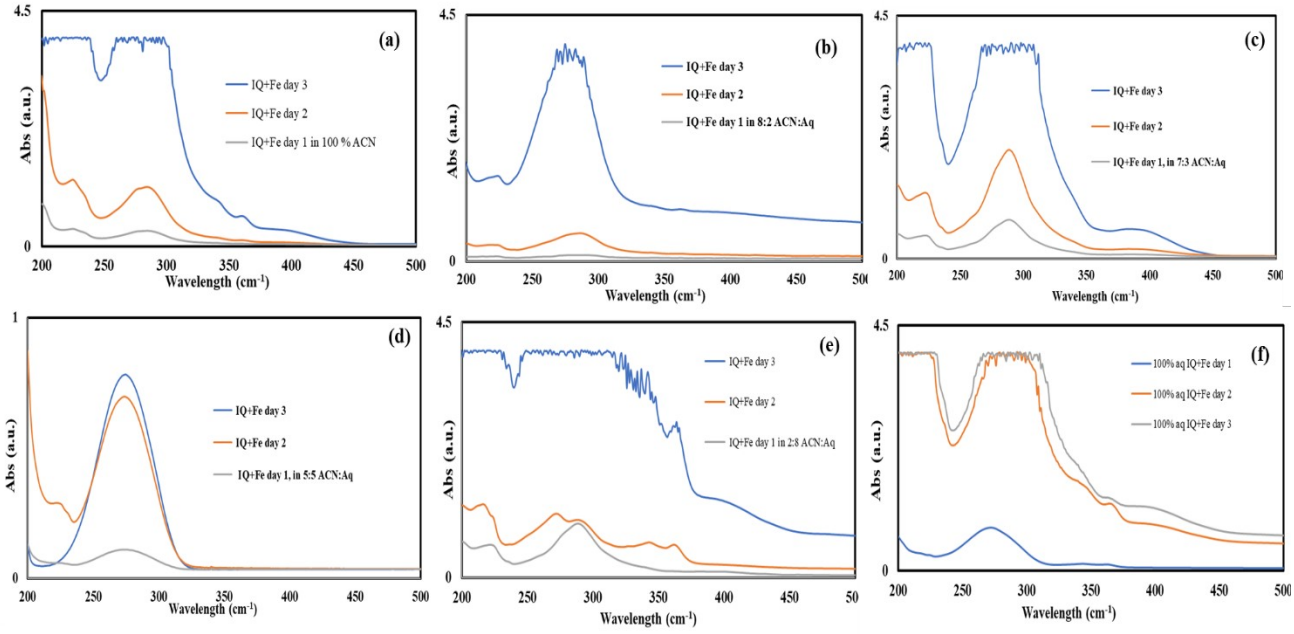

Fig S29. UV-Vis of IQ+Fe in **(a)** ACN, **(b)** 8:2, **(c)** 7:3, **(d)** 5:5, **(e)** 2:8 of ACN:aq solvent ratio and **(f)** aq, 1st, 2nd, and 3rd day.

(a)

EDX Report

Report No.

Sample Information

Sample Name	IQ FE 100%
Meas. Date	2023/04/06 15:14:39
Comment	Quick&easy Air-Metal
Group	easy
Operator	

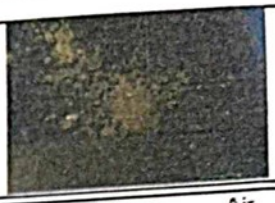

Measurement Condition

Channel	kV	uA	Filter	Acq.	Collimator	1mm	Atmos.	Air
Al-U	50	1000-Auto	----	0 - 40	Analysis	Time	DT%	
C-Sc	15	1000-Auto	----	0 - 20	0.00-40.00	Live- 30		14
					0.00- 4.40	Live- 30		3

Quantitative Result

Analyte	Result		Std.Dev.	Calc.Proc	Line	Intensity
Fe	91.493	%	[0.355]	Quan-FP	FeKa	20.3206
Si	4.024	%	[1.266]	Quan-FP	SiKa	0.0027
Zn	2.265	%	[0.067]	Quan-FP	ZnKa	0.3126
Ca	1.316	%	[0.144]	Quan-FP	CaKa	0.0226
S	0.650	%	[0.212]	Quan-FP	S Ka	0.0061
Mn	0.253	%	[0.026]	Quan-FP	MnKa	0.0540

Profile

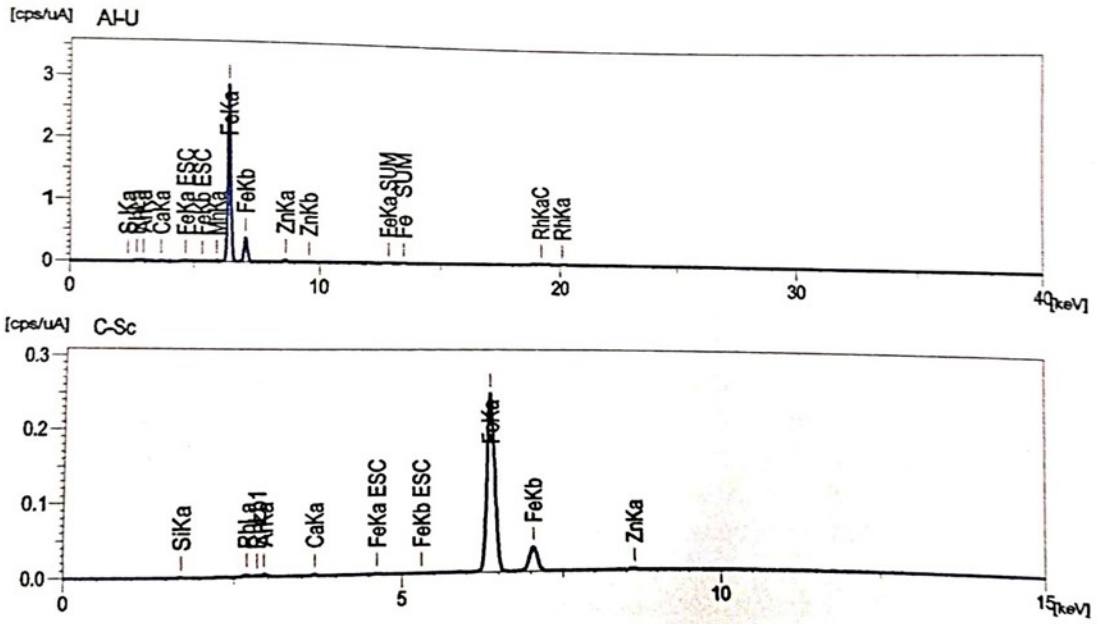

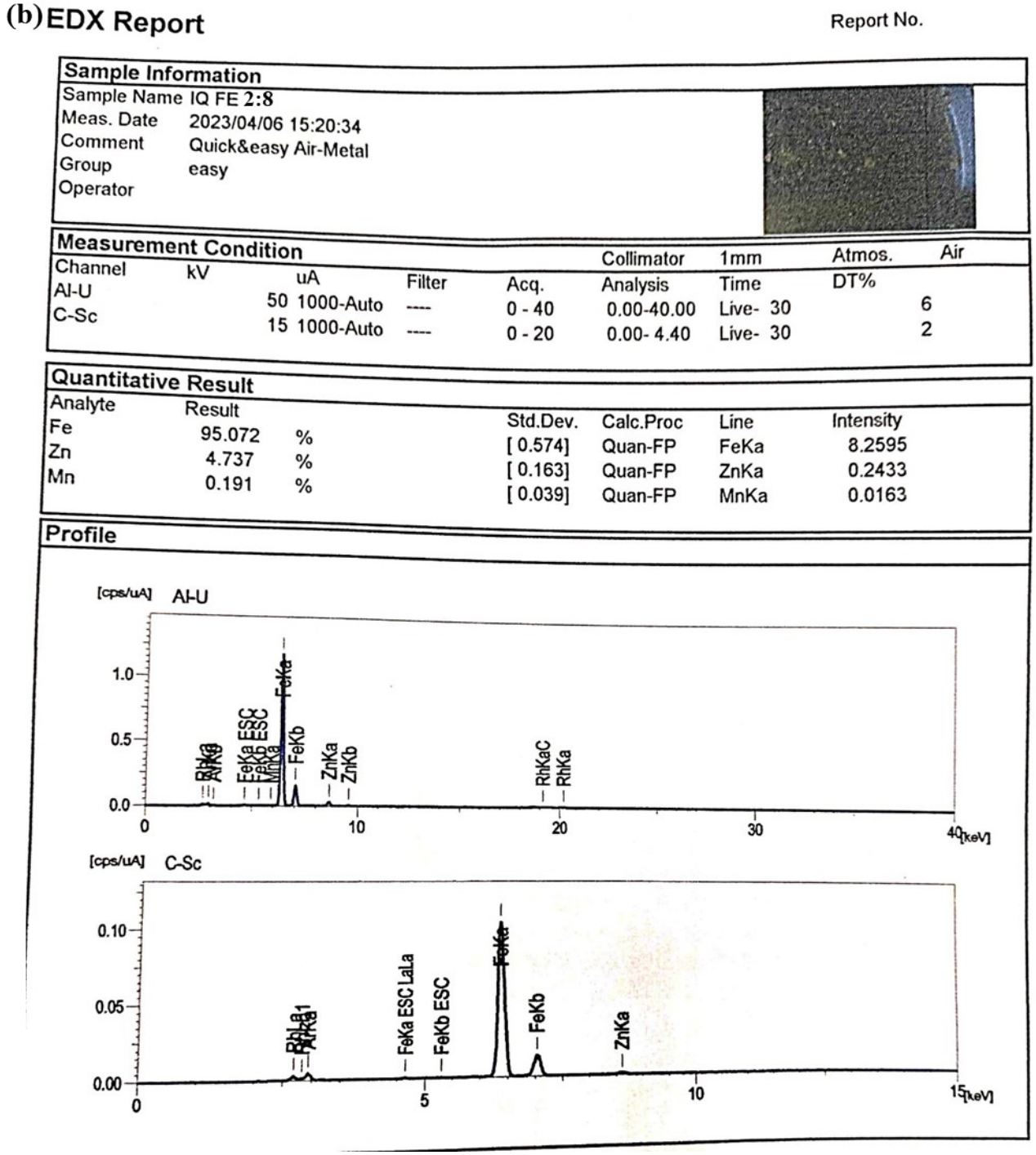

Fig S30. EDX spectra for IQ+Fe in **(a)** ACN and **(b)** 2:8 aq:ACN.

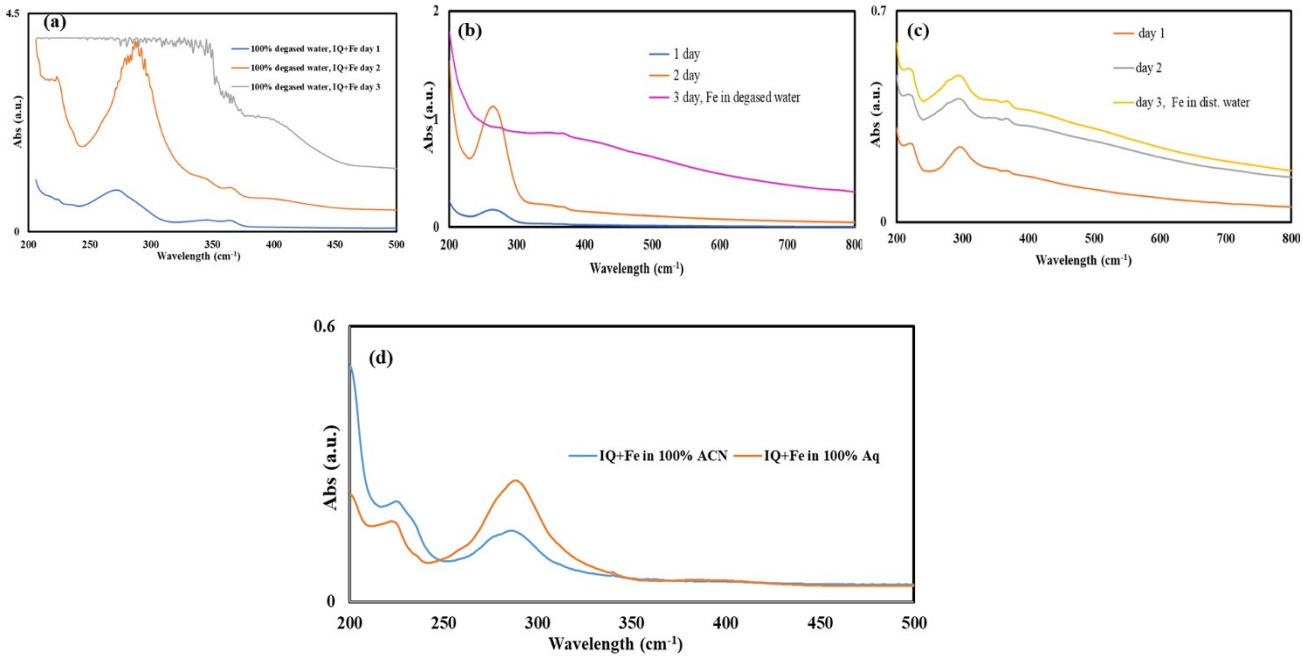

Fig S31. UV-Vis spectra for **(a)** IQ+Fe in degased water **(b)** only Fe in degased and distilled water on 1st, 2nd, and 3rd day **(c)** only IQ+Fe in distilled water and aq-ACN, and **(d)** IQ+Fe in ACN and aq.

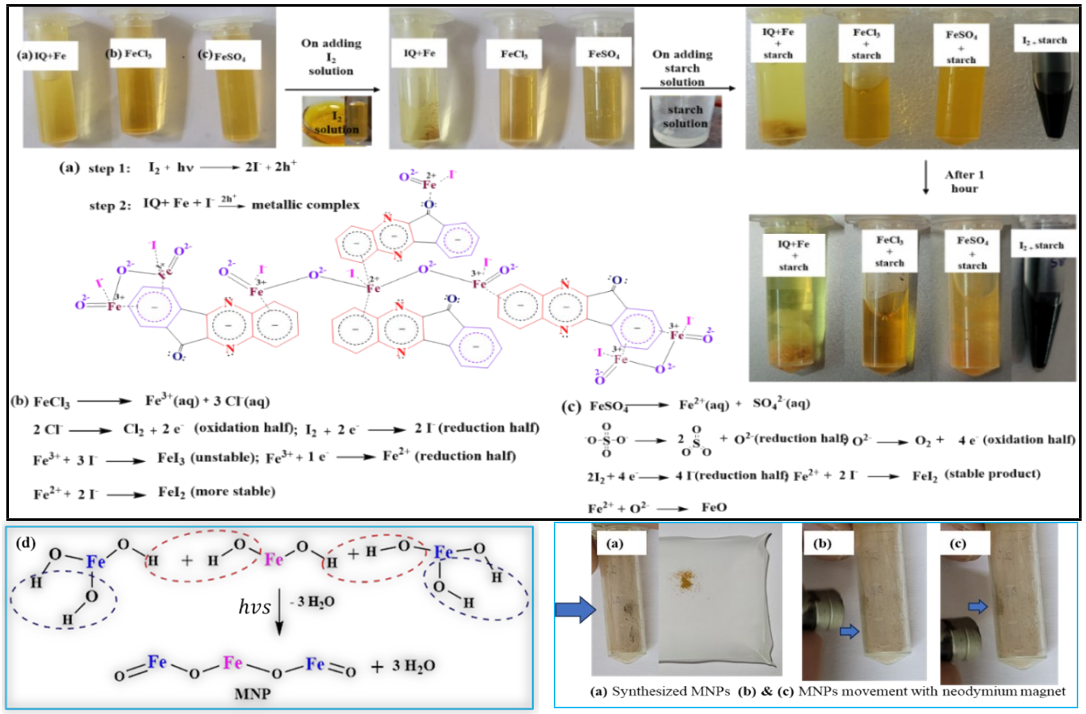

Fig. S32. (a) IQ+Fe, **(b)** aq $FeCl_3$, **(c)** aq $FeSO_4$ with iodine and starch solutions, and **(d)** IQ with Fe scrap synthesized MNPs.

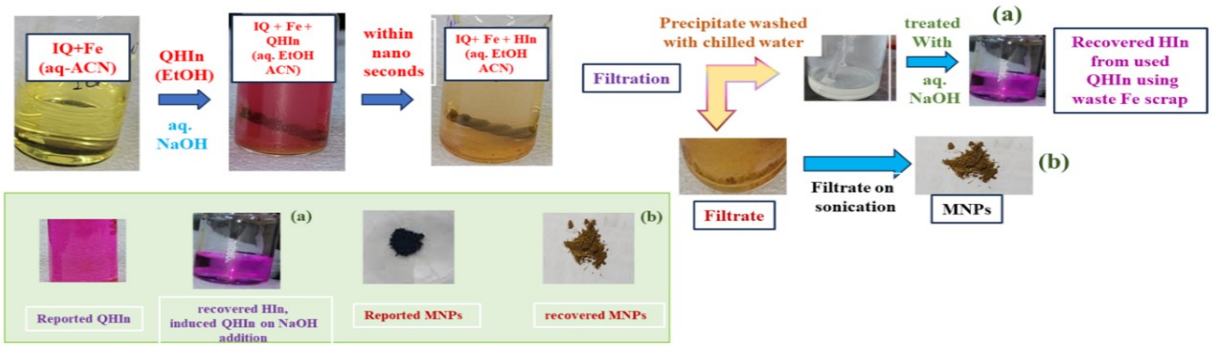

Fig. S33. Recovery of HIn from consumed QHIn by using waste Fe scrap.

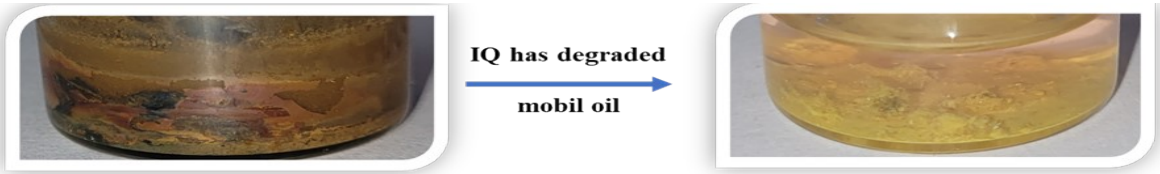

Fig. S34. IQ degraded mobil oil **(a)** initial and **(b)** after 15 days.

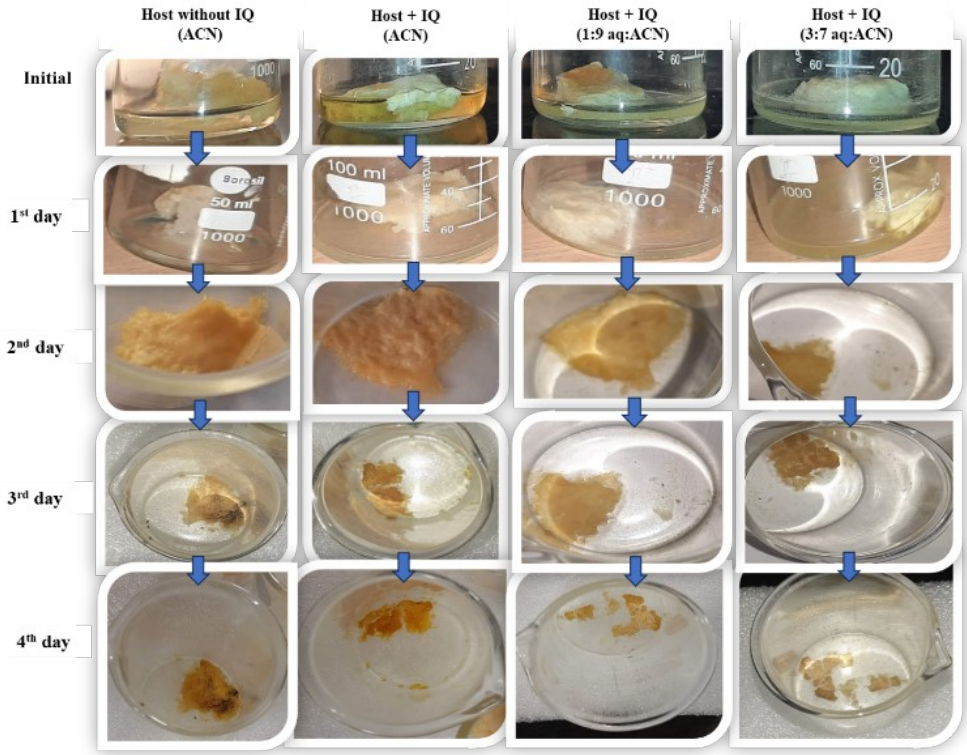

Fig. S35. Antifungal study of IQ with host.

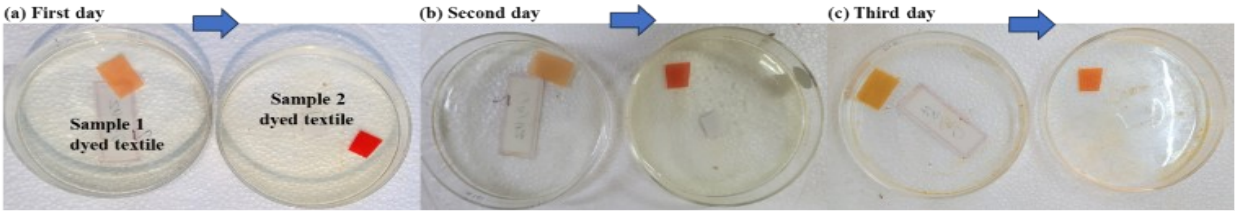

Fig. S36. Textile dye detachment using IQ.

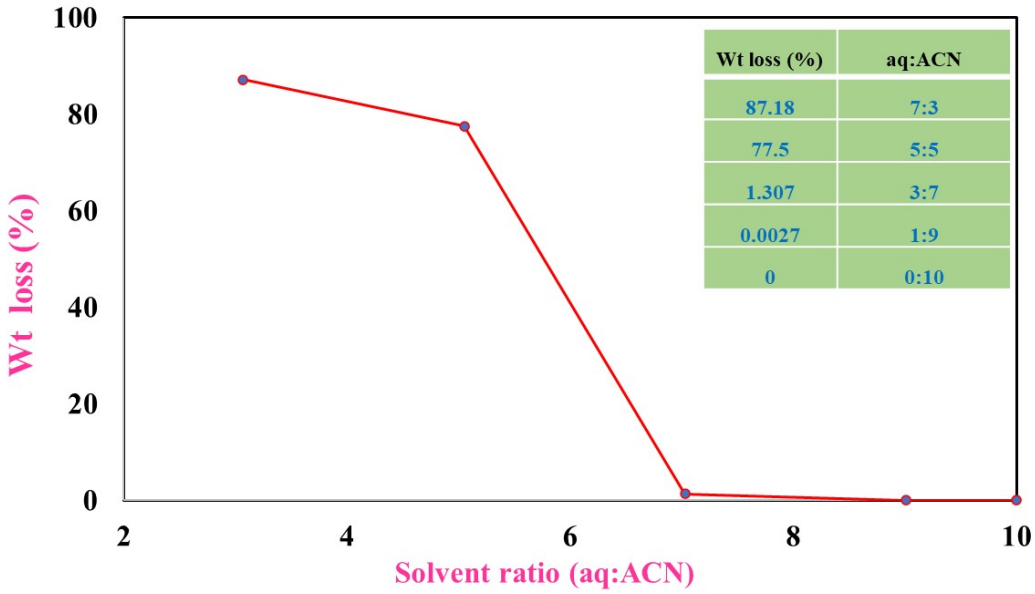

Chart S1. Rusting wt loss on varying solvent ratio of aq:ACN.

Table S8. IQ+Fe rusting effect in different ratios of aq:ACN.

Sr. no.	System	aq:ACN ratio	Initial wt of Fe (mg)	Final wt of Fe (mg)	Fe wt loss (%)
1	IQ+Fe	7:3	1207.17	1101.92	87.18
2	IQ+Fe	5:5	1202.19	1109.01	77.50
3	IQ+Fe	3:7	1199.07	1183.39	1.307
4	IQ+Fe	1:9	1466.05	1466.01	0.0027
5	IQ+Fe	water	1320.02	1320.02	$\sim 0 (nil)$

Table S9. Elemental analysis of IQ+Fe in ACN, 2:8 aq:ACN, 3:7 aq:ACN, and aq solvent ratios.

Sr. No.	Type	Name	N %	C %	H %	S %	O %
1	Std	Sulphanilamide	16.213	44.717	8.213	20.085	-
2	Std	Sulphanilamide	18.571	46.213	6.901	20.889	-
3	Std	Sulphanilamide	16.320	40.632	5.121	18.151	-
4	Std	Sulphanilamide	15.218	38.829	4.564	16.954	-
5	Std	Sulphanilamide	18.012	46.715	-	20.860	-
6	Std	Sulphanilamide	14.341	37.238	3.524	16.471	-
7	Smp	IQ+Fe in ACN	12.149	62.313	3.395	4.334	-
8	Smp	2:8 aq:ACN IQ+Fe	6.406	16.957	3.934	-	-
9	Smp	3:7 aq:ACN IQ+Fe	6.877	20.495	3.946	-	-
10	Smp	aq IQ+Fe	5.811	16.813	2.763	-	-

References

[1] R. Kumari and M. Singh, "Photocatalytic reduction of fluorescent dyes in sunlight by newly synthesized spiroindenoquinoxaline pyrrolizidines," *ACS Omega*, vol. 5, no. 36, pp. 23201–23218, Sep. 2020, doi: 10.1021/acsomega.0c02976.

[**2**] R. Kumari and M. Singh, "Spiroheterocyclic Photocatalyst for Reducing QHIn-Persistent Pollutants, Dyes, and Transition-Metal Ions Cocatalyzed with Electrolytes," *ACS Omega*, vol. 7, no. 44, pp. 40203–40229, doi: 10.1021/acsomega.2c05103.

[3] N. Kumar, C. Lal, B. Singh, and A. K. Patel, "Synthesis and Biological Activities of Some Novel Spiro Heterocyclic Pyrrolizidine Derivatives of 11H-indeno[1,2-b]quinoxaline through 1,3-Dipolar Cycloaddition," *Asian Journal of Chemistry*, vol. 32, no. 5, pp. 1255–1258, May 2020, doi: 10.14233/ajchem.2020.22630.